NASA TECHNICAL NOTE

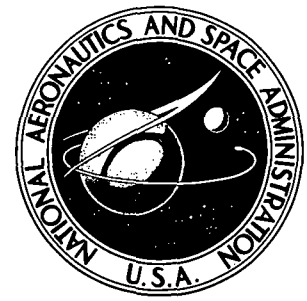

NASA TN D-7172

NASA TN D-7172

A FLIGHT INVESTIGATION OF THE TRAILING VORTICES GENERATED BY A JUMBO JET TRANSPORT

by Harry A. Verstynen, Jr., and R. Earl Dunham, Jr.

Langley Research Center
Hampton, Va. 23365

NATIONAL AERONAUTICS AND SPACE ADMINISTRATION • WASHINGTON, D. C. • APRIL 1973

1. Report No.	2. Government Accession No.	3. Recipient's Catalog No.
NASA TN D-7172		

4. Title and Subtitle	5. Report Date
A FLIGHT INVESTIGATION OF THE TRAILING VORTICES GENERATED BY A JUMBO JET TRANSPORT	April 1973
	6. Performing Organization Code
7. Author(s)	8. Performing Organization Report No.
Harry A. Verstynen, Jr., and R. Earl Dunham, Jr.	L-8706
	10. Work Unit No.
9. Performing Organization Name and Address	501-38-13-03
NASA Langley Research Center Hampton, Va. 23365	11. Contract or Grant No.
	13. Type of Report and Period Covered
12. Sponsoring Agency Name and Address	Technical Note
National Aeronautics and Space Administration Washington, D.C. 20546	14. Sponsoring Agency Code

15. Supplementary Notes

16. Abstract

A flight investigation has been conducted to study the velocity and persistence characteristics of the trailing vortices generated by a jumbo jet transport. The investigation showed that the tangential velocities were initially higher for vortices generated with the flaps up and that they persisted for longer distances behind the aircraft than those generated with the flaps down. The core radii with flaps down appeared to be generally larger than those with flaps up. The vertical locations of the vortices behind the generating aircraft varied from several hundred meters below the generating aircraft flight path at long ranges up to, and occasionally above, the flight path at short and moderate ranges.

17. Key Words (Suggested by Author(s))	18. Distribution Statement
Trailing vortices Wake turbulence Aircraft wakes	Unclassified – Unlimited

19. Security Classif. (of this report)	20. Security Classif. (of this page)	21. No. of Pages	22. Price*
Unclassified	Unclassified	44	$3.00

*For sale by the National Technical Information Service, Springfield, Virginia 22151

A FLIGHT INVESTIGATION OF THE TRAILING VORTICES GENERATED BY A JUMBO JET TRANSPORT

By Harry A. Verstynen, Jr., and R. Earl Dunham, Jr.
Langley Research Center

SUMMARY

A flight investigation has been conducted to study the velocity and persistence characteristics of the trailing vortices generated by a jumbo jet transport. The vortices were investigated at altitudes from about 1980 to 4600 meters, and at ranges behind the aircraft from 0.6 nautical mile to 13 nautical miles. The data showed that vortices generated with the flaps up exhibited velocities of approximately 17 m/sec at 1 minute of vortex age, 7 m/sec at 2 minutes age, and 2 m/sec at 3 minutes age. With the flaps down at the same ages, the vortices exhibited velocities of approximately 12 m/sec, 9 m/sec, and 8 m/sec. The vortices generated in the flap-up configuration had higher initial velocities and persisted for longer distances behind the generating aircraft than vortices generated in the flap-down configuration. Scatter in the core radius data precluded making quantitative comparisons between flap-up and flap-down configurations. In general, however, the flap-down core radii did appear to be larger than the flap-up radii of the same age. The vertical location of the vortices behind the generating aircraft varied from several hundred meters below the generating aircraft at long ranges up to, and occasionally above, the flight path at short and moderate ranges.

INTRODUCTION

A flight investigation has been conducted to determine the velocity, decay, and movement characteristics of the trailing vortices generated at altitude by a jumbo jet transport. (See table I.) The investigation was conducted as part of a general research program at the National Aeronautics and Space Administration to determine the general characteristics of trailing vortices and means for accelerating their breakup and decay. The investigation was conducted in cooperation with the United States Air Force Aeronautical Systems Command and the Air Force Flight Test Center. The tests were conducted in two parts; the first series in the vicinity of Wright-Patterson Air Force Base, Ohio (test area A), and the second series in the vicinity of Edwards Air Force Base, California (test area B). The tests consisted of flying an instrumented T-33 aircraft through the vortices of the jumbo aircraft using the entrainment of the smoke normally

generated by the engines to define the locations of the vortices. The technique employed in acquisition and reduction of the data is similar to that used in previous investigations of trailing vortices (ref. 1) and atmospheric turbulence (ref. 2), respectively.

The results of these tests are presented herein in terms of three-component vortex velocity plots, vortex spacing data, vortex location data, and decay curves for maximum velocity and core radius. The results include data taken in both flap-up and flap-down configurations at low speeds. Part of the data presented in this report was previously reported in reference 3.

SYMBOLS

Measurements and calculations were made in the U.S. Customary Units. They are presented herein in the International System of Units (SI).

$\vec{a}$	acceleration vector measured along aircraft longitudinal, lateral, and normal body axes, m/sec^2
b	aircraft wing span, m
b'	theoretical vortex core spacing, $\frac{\pi b}{4}$, m
$\vec{b}$	bias vector chosen to make gust velocities zero at end of run
$\vec{d}$	distance from flow vanes to aircraft center of gravity, m
g	acceleration due to gravity, 9.8 m/sec^2
Δh	measured vertical position of trailing vortex relative to generating aircraft, m
$\Delta h'$	measured vertical position of trailing vortex relative to generating aircraft normalized with respect to circulation and true airspeed, m
$\Delta h'_{av}$	predicted vertical position of trailing vortex relative to generating aircraft based on average values of circulation and true airspeed, m
$\vec{i},\vec{j},\vec{k}$	unit vectors
p,q,r	aircraft roll, pitch, and yaw rates, respectively, rad/sec

r_c	radius of vortex core, m
S	separation distance between generating and probe aircraft, m
$\frac{S}{\sqrt{t\Gamma_o}}$	nondimensional separation distance
t	vortex age, sec
t'	time, sec
u,v,w	vortex velocity components along the inertial X, Y, and Z axes, respectively, m/sec
V_{av}	average airspeed, m/sec
V_o	aircraft true airspeed, m/sec
V_θ	tangential velocity, m/sec
$V_{\theta,m}$	maximum tangential velocity, m/sec
$\frac{V_{\theta,m}}{V_o}$	nondimensional vortex maximum tangential velocity
W	aircraft weight, N
W_{av}	average aircraft weight, N
X,Y,Z	inertial or earth-fixed axes
2y'	distance between peaks on tangential velocity plot for core penetrations
α	angle of attack sensed by flow vanes, rad
β	angle of sideslip sensed by flow vanes, rad

Γ_{av} average circulation, $\frac{4W_{av}}{\pi b \rho_{av} V_{av}}$ (462.6 m^2/sec for flap-up configuration; 591.8 m^2/sec for flap-down configuration)

Γ_o circulation, $\frac{4W}{\pi b \rho V_o}$, m^2/sec

δ angle between tangential velocity vector and the inertial Z-axis

θ, ϕ, ψ Euler angles between body and inertial reference frames, rad

ν eddy viscosity, m^2/sec

ρ ambient air density, kg/m^3

ρ_{av} average ambient air density, kg/m^3

$\vec{\omega}$ angular velocity of the aircraft, $p\vec{i} + q\vec{j} + r\vec{k}$, rad/sec

INSTRUMENTATION

The T-33 probe aircraft (fig. 1) was instrumented to record in analog form on oscillograph flight recorders airspeed, altitude, angle of attack, angle of sideslip, total temperature, accelerations of the center of gravity along the three aircraft body axes, rotational rates about the three body axes, aircraft attitude changes relative to inertial axes, and air-to-air range.

During the tests in test area A, the aircraft was equipped with a nose-boom-mounted pitot-static system (independent of the aircraft's system) to make accurate airspeed measurements. However, for the tests in test area B, this system was replaced by a total-pressure system which measured changes in total pressure relative to a fixed reference pressure. This substitution was made because the damping of the pitot-static system was found to be less than desirable for making vortex measurements (approximately 0.38). Wind-tunnel tests of the balsa wood vanes used to measure flow-field angularity indicated that the response characteristics of the vanes could be closely approximated by single-degree-of-freedom second-order systems where the damping ratio was a function of density and the natural frequency was a function of dynamic pressure. (See ref. 4.) The dynamic characteristics of the sensors installed in the T-33 probe aircraft are presented in table II.

TESTS

The T-33 probe aircraft was flown through the vortex field of the generating aircraft by viewing the engine smoke to define the locations of the vortices. The tests were conducted with the generating aircraft in both the cruise (flap-up) configuration and the landing (flap-down) configuration, at several altitudes at low speeds. (See table III.) The weight of the generating aircraft ranged from 1 703 700 N to 2 735 600 N during the tests. A survey of angle of attack and accelerometer readings taken during runs with the probe aircraft in level unaccelerated flight at the test altitude indicated that the tests were conducted in smooth-air conditions. There was, however, some evidence of large-scale convective activity in test area A, as will be pointed out later in the report. Temperature profiles for the two test areas taken with the probe aircraft indicated lapse rates in both areas were between -3.5° C/km and -7.3° C/km.

DATA REDUCTION

Although considerable effort was expended to insure accurate instrumentation, it was necessary to employ special filters to compensate partially for the second-order dynamics of the flow vanes and airspeed system, and to fair the raw data manually to suppress boom bending effects in the vane deflections. The flow-vane measurements were referenced to a set of fixed earth axes, or inertial axes, by correcting them for aircraft motions by the use of a computer routine to solve the following equation:

$$\begin{Bmatrix} u \\ v \\ w \end{Bmatrix} = -\{T\}\{V_{Vanes}\} + \{T\}\{\vec{\omega} \times \vec{d}\} + \int_0^{t'} \{T\}\left[\{\vec{a} - \vec{b}\} - \{T\}^{-1}\begin{Bmatrix} 0 \\ 0 \\ g \end{Bmatrix}\right] dt'$$

$$+ \left[\{T\}\{V_{Vanes}\} - \{T\}\{\vec{\omega} \times \vec{d}\}\right]_{t'=0}$$

The matrix $\{T\}$ is the transformation matrix to convert measurements made in the aircraft body axes to measurements in an inertial reference frame. This matrix as given in reference 5 is

$$\{T\} = \begin{Bmatrix} (\cos\psi\cos\theta) & (\cos\psi\sin\theta\sin\phi - \sin\psi\cos\phi) & (\cos\psi\sin\theta\cos\phi + \sin\psi\sin\phi) \\ (\sin\psi\cos\theta) & (\sin\psi\sin\theta\sin\phi + \cos\psi\cos\phi) & (\sin\psi\sin\theta\cos\phi - \cos\psi\sin\phi) \\ (-\sin\theta) & (\cos\theta\sin\phi) & (\cos\theta\cos\phi) \end{Bmatrix}$$

The vector $\vec{b}$ is a bias which was applied to the acceleration vector to drive the vortex velocity components to zero at the end of each run. The origin of the inertial reference frame for each vortex penetration was the point in space at which the data-recording system was activated. The orientation of the axes was such that the positive X inertial axis was alined azimuthally with the generating aircraft heading and the positive Z inertial axis was normal to the earth and pointing downward.

The matrix $\{V_{Vanes}\}$ represents the flow-field angularity at the nose of the aircraft, as sensed by the angle-of-attack and angle-of-sideslip vanes and combined with the airspeed sensed by the total-pressure system. This matrix includes both the effects of the motion of the vanes through the atmosphere and the motions imposed on the vanes by the vortex, and can be expressed as

$$\{V_{Vanes}\} = \begin{Bmatrix} V_o \cos \alpha \cos \beta \\ V_o \sin \beta \\ V_o \sin \alpha \end{Bmatrix}$$

In order to evaluate the accuracy of the total data acquisition and reduction technique, the T-33 probe aircraft was run through a series of maneuvers in calm air. The velocities resulting from the reduction of this data by the vortex data reduction program were attributed to inaccuracies in the aircraft's instrumentation and/or the data reduction process. Based on this type of analysis, it is felt that the accuracy of the final velocities is approximately ± 1 to ± 2 m/sec. Computer simulations of the response of the angle-of-attack vane to penetrations of a simulated vortex core indicate that the minimum core radius that could be detected was about 0.8 meter.

DATA ANALYSIS

Plots of the longitudinal, lateral, and vertical velocity components against lateral distance through the vortex for 20 penetrations are presented in figures 2 and 3. Figure 2 represents vortices generated in the flap-up configuration and figure 3 represents vortices generated in the flap-down configuration. The technique used to determine whether a particular velocity profile represented a core penetration was to generate a plot of tangential velocity against distance through the vortex by taking the vector sum of the lateral and vertical velocities at each point through the vortex. The vertical-velocity component was adjusted for the effect of one vortex on the other by displacing the $w = 0$ line to a point halfway between the positive and negative vertical peaks. The lateral-velocity component was corrected for an apparent lag in the total-pressure system by shifting the velocity profile along the distance axis so that the peak lateral velocity

occurred when the vertical velocity was passing through zero. These corrections, which are illustrated in sketch (a), were used for analysis only and are not reflected in the data of figures 2 and 3.

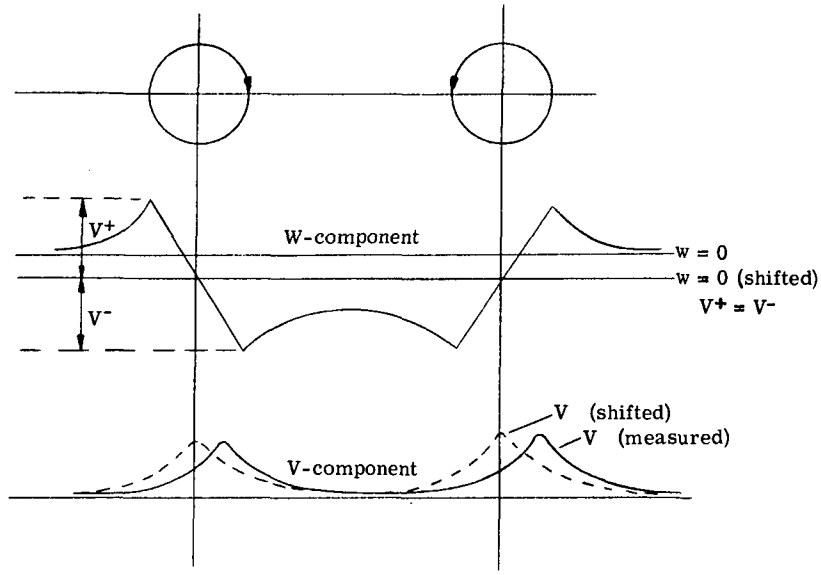

Sketch (a)

These corrections were incorporated before the tangential velocity profile was computed. Depending upon whether the tangential velocity profile generated had two peaks or one peak per vortex, the vortex penetration was classified as core or noncore, respectively. Those vortices which exhibited the single peak characteristic of a noncore penetration but velocities very near those for core penetrations of similar age were classified as near-core penetrations.

In order to determine the radius of the core once a particular vortex was classified as a core penetration, a graphical technique illustrated in figure 4 was utilized. The distance y' was found by taking half the difference in distance between the peaks of the tangential velocity plot. This distance was multiplied by the ratio of the maximum tangential velocity to the vertical velocity at the same time to correct for offset of the flight path relative to the core center line. Core radii determined in this manner are presented in table III.

Both the classification of core penetrations and the determination of core radius are based on the classical vortex model which depicts the vortex as having a region of solid body rotation in the center and a region of induced flow outside the solid region. The region inside is known as the core and has the property that the tangential velocity varies directly with radius, whereas in the outside region the velocity varies inversely with radius.

The distance between the right and left vortices, or vortex spacing, and the vertical locations of the vortices behind the generating aircraft, or vortex positions, were determined from plots similar to the sample plot presented as figure 5. By following a procedure developed by Kraft in reference 1, the tangential velocity vectors were plotted for each data point through the vortex and a perpendicular to the vectors drawn. The intersections of the perpendiculars were taken as the centers of the vortices and the vortex spacing was taken as the distance between the intersections. The vertical position of the vortex was taken as the altitude difference between the generating aircraft when it generated a particular vortex segment and the probe aircraft when it penetrated that segment, corrected for the displacement of the T-33 flight path relative to the vortex center line as determined from the vector plot. Since it was not necessary that the maximum velocity in the vortex be measured for the vortex spacing and position information to be useful, all penetrations which gave reasonable intersections were used in analyzing the spacing and position data.

RESULTS AND DISCUSSION

During the tests 346 penetrations of the vortex flow field were attempted and they provided 55 penetrations which gave responses warranting further analysis. Of these 55 penetrations, 12 were penetrations of the vortex core and 8 others appeared to have passed near the core. Of the 20 core and near-core penetrations, 6 were with the generating aircraft in the flap-up configuration and 14 were with the generating aircraft in the flap-down configuration. The poor percentage of core penetrations relative to the total number of attempts is attributed to a combination of very small cores and poor definition of the vortices by normal engine smoke. The use of this technique is not recommended for future research unless a better scheme is found for defining the locations of the vortices at long ranges. However, even with better definition of the vortices, considerable flight time may be required to obtain a useful number of core penetrations because of the variability in core location and core size observed during these tests.

The spacing of the vortices as a function of distance behind the aircraft is illustrated in figure 6. Analysis of these data seems to indicate that the vortices are separated by a distance of about 48 meters or 71 percent of the generating aircraft span out to a range of about 4 nautical miles. Beyond this range, the flap-down vortices seem to exhibit somewhat erratic behavior. This behavior might be attributable to the interaction of atmospheric turbulence with the vortices, the action of a natural oscillatory instability in the vortices, or both. Definite conclusions about the behavior of the flap-up vortices cannot be drawn because of the lack of data between 4 and 6 nautical miles. The measured spacing of 71 percent compares well with the 78.6-percent value predicted in reference 6.

Figure 7 illustrates the vertical position of the vortices as a function of distance behind the generating aircraft for the flap-up and flap-down configurations. The lines show the position of the vortices that were predicted by two-dimensional, irrotational, incompressible vortex theory. (See ref. 7.) These data have been normalized with respect to average circulation and average true airspeed to make the data for different flight conditions directly comparable with each other and with the theoretical formulation. In the flap-up configuration, the vertical locations of the vortex varied from approximately 180 meters below the generating aircraft flight path at long ranges up to and occasionally above the flight path at short and moderate ranges. In the flap-down configuration, the vertical locations varied from approximately 330 meters below the generating aircraft flight path at moderate ranges to 40 meters below the flight path at short ranges.

As shown in figure 7(a), the vortices measured in test area A exhibited behavior somewhat different from those measured in test area B. The vortices for test area A seem to fall well above the predicted location and at times even above the flight path of the generating aircraft. In test area B, the vortices seem to fall nearer the predicted line. A possible explanation for this difference in behavior would be that convective activity in test area A affected the vortices but was of sufficiently large scale that it could not be detected by the normal accelerometer or angle-of-attack vane of the probe aircraft. This explanation is not inconceivable when it is considered that the tests were run at lower altitudes in test area A where convective activity is generally stronger and that test area A had significantly more clouds near the test altitude than test area B. Figure 7(a) also shows that the vortices measured in test area B had a tendency to level off at long ranges. This tendency could be the result of the measurements being taken at the tops of vertical oscillations of the vortices or the descent rate of the vortices decreasing as the tangential velocity in the vortices decayed. In any case, the leveling off seems to be consistent with the results for two other aircraft presented in reference 8.

Figure 7(b) shows that the vortices measured in test area B with the flaps down did not exhibit the leveling-off tendency but tended to scatter about the locations predicted by the theoretical formulation. Measurements, however, were not obtained at the long ranges where the flap-up vortices tended to level off.

The measured variation of maximum tangential velocity with vortex age is shown in figure 8(a) (flap-up configuration) and figure 8(b) (flap-down configuration) by the symbols and dashed lines. The vortex age t was determined by dividing the separation distance, as recorded at the time of penetration, by the true airspeed of the generating aircraft. The airspeed of the generating aircraft was held constant during each run. Note that the maximum tangential velocity has been adjusted for differences in weight, speed, span, and altitude by the circulation ratio Γ_{av}/Γ_o, where Γ_{av} represents the average flight condition for that configuration. The dashed curves represent a reasonable fairing of the data and all discussions will be based on these curves.

A number of researchers have proposed that the decay of maximum vortex velocity with vortex age should follow the general form of the equation developed by Lamb in reference 6 for a viscous vortex with circulation constant with age, but with the kinematic viscosity term replaced by an empirically determined eddy viscosity which accounts for the turbulence in the atmosphere and the turbulence in the boundary layer of the wing. (See, for example, refs. 9 and 10.) By following this approach, a family of curves generated by substituting several different values of eddy viscosity into Lamb's viscous decay equation are plotted in figures 8(a) and 8(b) for comparison. Analysis of these figures indicates that the flap-up vortices decay at a greater rate than was predicted by the eddy-viscosity model, whereas the flap-down vortices decay at about the viscous rate when the eddy-viscosity factor has a value of about 0.1 m^2/sec. Of course, the previously mentioned effect of atmospheric conditions on vortex locations could also significantly affect vortex decay rates.

In terms of actual velocities, the data showed that vortices generated with flaps up $\left(\Gamma_{av} = 463\ m^2/sec\right)$ exhibited velocities of approximately 17 m/sec at 1 minute of age, 7 m/sec at 2 minutes age, and 2 m/sec at 3 minutes age. Vortices generated with the flaps down $\left(\Gamma_{av} = 592\ m^2/sec\right)$ exhibited velocities of about 12 m/sec, 9 m/sec, and 8 m/sec at the same ages. The large differences in average circulation and the different nominal airspeeds associated with the flap-up and flap-down configurations prevented making direct comparisons of vortex persistence on the basis of vortex age. The data of figure 8 were therefore replotted as a function of nondimensional distance in figure 9. The nondimensional distance parameter was based on Squire's work in reference 11 which assumes that eddy viscosity is directly proportional to circulation. The curves represent a reasonable fairing of the data. When plotted in this form, the data indicate that the vortices generated in the flap-up configuration persist for longer distances behind the generating aircraft than those generated in the flap-down configuration. This result is consistent with the results of reference 12.

Figures 10(a) and 10(b) are plots of the vortex core radius as a function of vortex age for flap-up and flap-down configurations, respectively. Also shown in the figure are curves representing the core radius against time relationship predicted by the same eddy-viscosity model discussed in figure 8. Each line represents a different value of eddy viscosity. The data in figures 10(a) and 10(b) indicate that the core radius increases generally with time and that the flap-down radii are generally larger than the flap-up radii. The scatter and small amount of data obtained preclude definition of the exact variation with time. Note that the value of ν which gives a good fit to the data of figure 8(b) does not give a good fit to the core radius data of figure 10(b).

Two points of figure 10(b) are deserving of special attention – the points at 60 seconds and 63 seconds, which show unusually large core radii compared with most of the

data. The most probable explanation for this behavior is that these two runs penetrated vortex segments which had already broken up. Reference to figure 8(b) also suggests that the vortex may have been breaking up since the velocities measured on these two runs are slightly lower than those for the rest of the data.

The vortices generated by the jumbo jet used in this investigation were observed to undergo the oscillatory instability noted by many other observers. However, a lack of clear definition of the vortices by engine smoke precluded the observation of the actual breaking up of the vortices. Previous studies have indicated, however, that the oscillatory instability tends to grow in amplitude until a break finally occurs, usually where the two vortices touch. It is felt that this natural breaking up process, together with the effect of the interaction of the vortices with atmospheric turbulence and convective activity, could be responsible for much of the scatter observed in the data.

SUMMARY OF RESULTS

An investigation was made to determine the characteristics of the trailing vortices generated by a jumbo jet aircraft. These measurements were made by flying an instrumented T-33 aircraft in the wake of the jumbo jet at separation distances from 0.6 to 13 nautical miles. Analysis of the data revealed the following general characteristics:

1. The distance between vortex centers appears to stay relatively constant at 71 percent of the aircraft span out to a range of approximately 4 nautical miles for vortices generated in both flap-up and flap-down configurations. Beyond this range, the flap-down vortices exhibit considerable scatter. The separation predicted theoretically is 78.6 percent of the aircraft span.

2. The vertical locations of the vortices varied from approximately 180 meters below the jumbo jet flight path at long ranges up to, and occasionally above, the flight path at short and moderate ranges with the jumbo jet in a flap-up configuration. With the flaps down, the vortices were found from about 330 meters below the flight path at moderate ranges to about 40 meters below at short ranges. The data compares reasonably well with the vertical locations predicted theoretically, although atmospheric conditions appeared to have some effect on these locations.

3. The tangential velocities in vortices generated with the flaps up were about 17 m/sec at 1 minute vortex age, 9 m/sec at 2 minutes age, and 2 m/sec at 3 minutes age. Flap-down vortices of the same ages had tangential velocities of 12 m/sec, 9 m/sec, and 8 m/sec.

4. The data were found to be inconsistent with theoretically predicted values of maximum tangential velocity and core radius for a single value of eddy viscosity and constant circulation.

5. Vortices generated in the flap-up configuration persist for longer distances behind the generating aircraft and have higher velocities at a given age than vortices generated in the flap-down configuration.

6. The radius of the vortex core for both flap-up and flap-down vortices shows a general increase with time. The flap-down radii appear to be generally larger than the flap-up radii, but scatter in the data due primarily to variability of the vortex core precludes making quantitative comparisons.

7. The technique employed in this investigation of penetrating trailing vortices at altitude with an instrumented aircraft was found to require considerable flight time to acquire very small quantities of useful data. Any further studies employing this technique should be attempted only if a good technique for defining vortex locations at long ranges is available. However, even with good definition of the vortex locations, considerable flight time may still be required to obtain a useful number of core penetrations because of the high variability of the core locations and size.

Langley Research Center,
National Aeronautics and Space Administration,
Hampton, Va., April 3, 1973.

REFERENCES

1. Kraft, Christopher C., Jr.: Flight Measurements of the Velocity Distribution and Persistence of the Trailing Vortices of an Airplane. NACA TN 3377, 1955.

2. Monson, K. R.; Jones, G. W.; Mielke, R. H.; et al.: Low Altitude Atmospheric Turbulence Lo-Locat Phase III Interim Report. Vol. II. Instrumentation and Data Processing Details, Gust Velocity Data, and Test Log. AFFDL-TR-69-63, Vol. II, U.S. Air Force, Oct. 1969.

3. Dunham, R. Earl, Jr.; Verstynen, Harry A., Jr.; and Benner, Margaret S.: Progress Report on Wing-Trailing-Vortex Studies. NASA Aircraft Safety and Operating Problems, Vol. I, NASA SP-270, 1971, pp. 101-113.

4. Richardson, Norman R.: Dynamic and Static Wind-Tunnel Tests of a Flow-Direction Vane. NASA TN D-6193, 1971.

5. Anon.: Fundamentals of Design of Piloted Aircraft Flight Control Systems. Vol. II. Dynamics of the Airframe. BuAer Rep. AE-61-4, Bur. Aeronaut., Feb. 1953.

6. Spreiter, John R.; and Sacks, Alvin H.: The Rolling Up of the Trailing Vortex Sheet and Its Effect on the Downwash Behind Wings. J. Aeronaut. Sci., vol. 18, no. 1, Jan. 1951, pp. 21-32, 72.

7. Lamb, Horace: Hydrodynamics. Sixth ed., Cambridge Univ. Press, 1932.

8. Tracy, Peter W.: Results of the Boeing Company Wake Turbulence Test Program. Doc. No. D6-30851, Boeing Co., 1970.

9. Bleviss, Zegmund O.: Theoretical Analysis of Light Plane Landing and Take-Off Accidents Due to Encountering the Wakes of Large Airplanes. Rep. No. SM-18647, Douglas Aircraft Co., Inc., Dec. 1954.

10. Kerr, T. H.; and Dee, F.: A Flight Investigation Into the Persistence of Trailing Vortices Behind Large Aircraft. Technical Note No. Aero. 2649, British R.A.E., Sept. 1959.

11. Squire, H. B.: The Growth of a Vortex in Turbulent Flow. Rep. No. F.M. 2053, Brit. A.R.C., Mar. 18, 1954.

12. Andrews, William H.; Robinson, Glenn H.; and Larson, Richard R.: Exploratory Flight Investigation of Aircraft Response to the Wing Vortex Wake Generated by Jet Transport Aircraft. NASA TN D-6655, 1972.

TABLE I.- JUMBO-JET CHARACTERISTICS

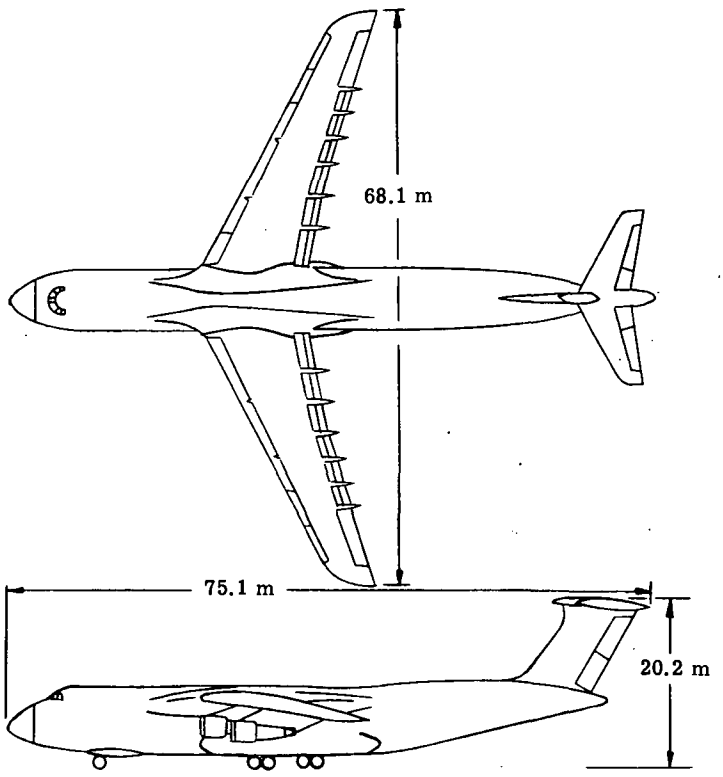

Normal gross weight, N	3 255 924
Empty weight, N	1 422 996
Average chord, m	8.58
Wing area, m^2	577
High-lift devices	Double-slotted Fowler flaps; leading-edge slats

TABLE II.- INSTRUMENT RESPONSE CHARACTERISTICS

Sensor	Approximate damping ratio	Approximate natural frequency, Hz
Angle of attack*	0.625	46
Angle of sideslip*	0.625	46
Pitot static (boom-mount)	0.2	13
Total pressure	0.575	28
Accelerometers	0.70	1200
Rate gyros	0.6	23
Nose boom (test area A)	0.01	10
Nose boom (test area B)	0.07	13

*These values are for an altitude of 3658 meters and an indicated airspeed of 230 knots.

TABLE III.- TABULATED DATA

Figure	Flaps	Weight, N	True airspeed, m/sec	Altitude, m	Γ_o, m^2/sec	Vortex age, sec	r_c, m	V_θ,m, m/sec
2(a)	Up	1.8727×10^6	97.8	1981	356.0	46	0.783	18.0
2(b)	Up	2.2641	115.3	4578	477.8	60		14.4
2(c)	Up	2.5639	107.6	3652	526.3	98	1.94	12.9
2(d)	Up	1.7037	98.8	2295	330.5	104	2.81	4.8
2(e)	Up	2.7356	122.0	4572	544.9	163		5.3
2(f)	Up	2.7072	122.0	4572	539.9	198	2.57	1.7
3(a)	Down	2.1898	84.4	4572	631.3	24	2.05	16.8
3(b)	Down	2.0066	89.1	4572	548.0	59	1.77	11.0
3(c)	Down	2.0061	83.5	4596	582.9	60	4.87	9.38
3(d)	Down	2.3202	95.7	4572	589.9	63	9.7	8.14
3(e)	Down	2.3171	95.7	4572	589.1	78	2.74	11.8
3(f)	Down	2.3500	95.7	4572	597.5	82	2.03	9.9
3(g)	Down	2.1827	84.4	4578	629.3	85		10.7
3(h)	Down	2.0044	83.4	4596	584.8	92		10.1
3(i)	Down	1.9888	83.4	4581	580.2	93	2.18	8.9
3(j)	Down	2.1342	84.9	4578	611.7	106		11.9
3(k)	Down	1.9407	83.9	4587	562.8	109		10.8
3(l)	Down	2.3117	95.7	4572	587.8	115		8.8
3(m)	Down	2.3411	95.7	4572	595.2	133	4.49	8.3
3(n)	Down	2.3375	95.7	4572	594.3	147		7.7

L-71-1804

Figure 1.- T-33 probe aircraft.

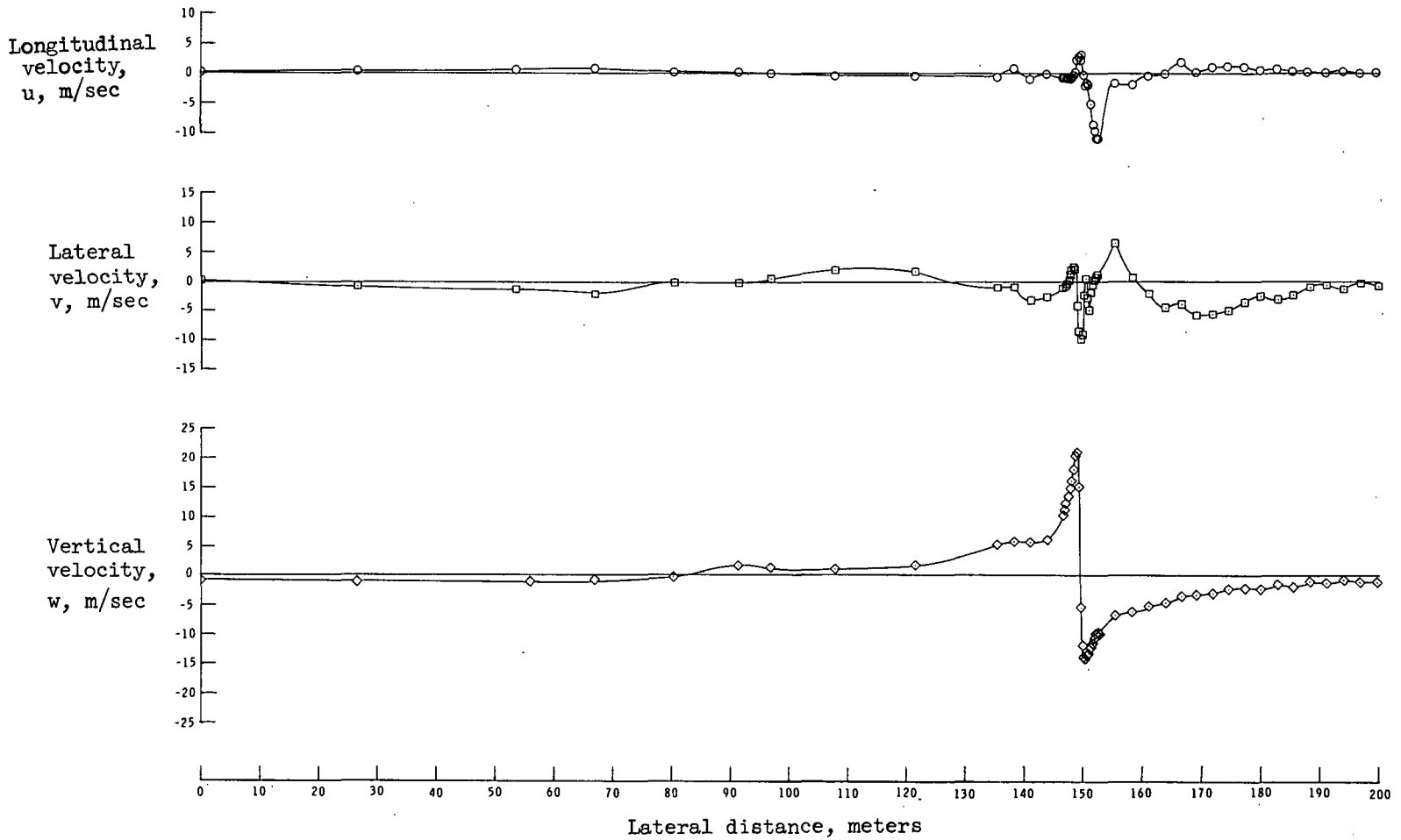

(a) t = 46 sec.

Figure 2.- Vortex velocity component variation with lateral distance. Flaps up.

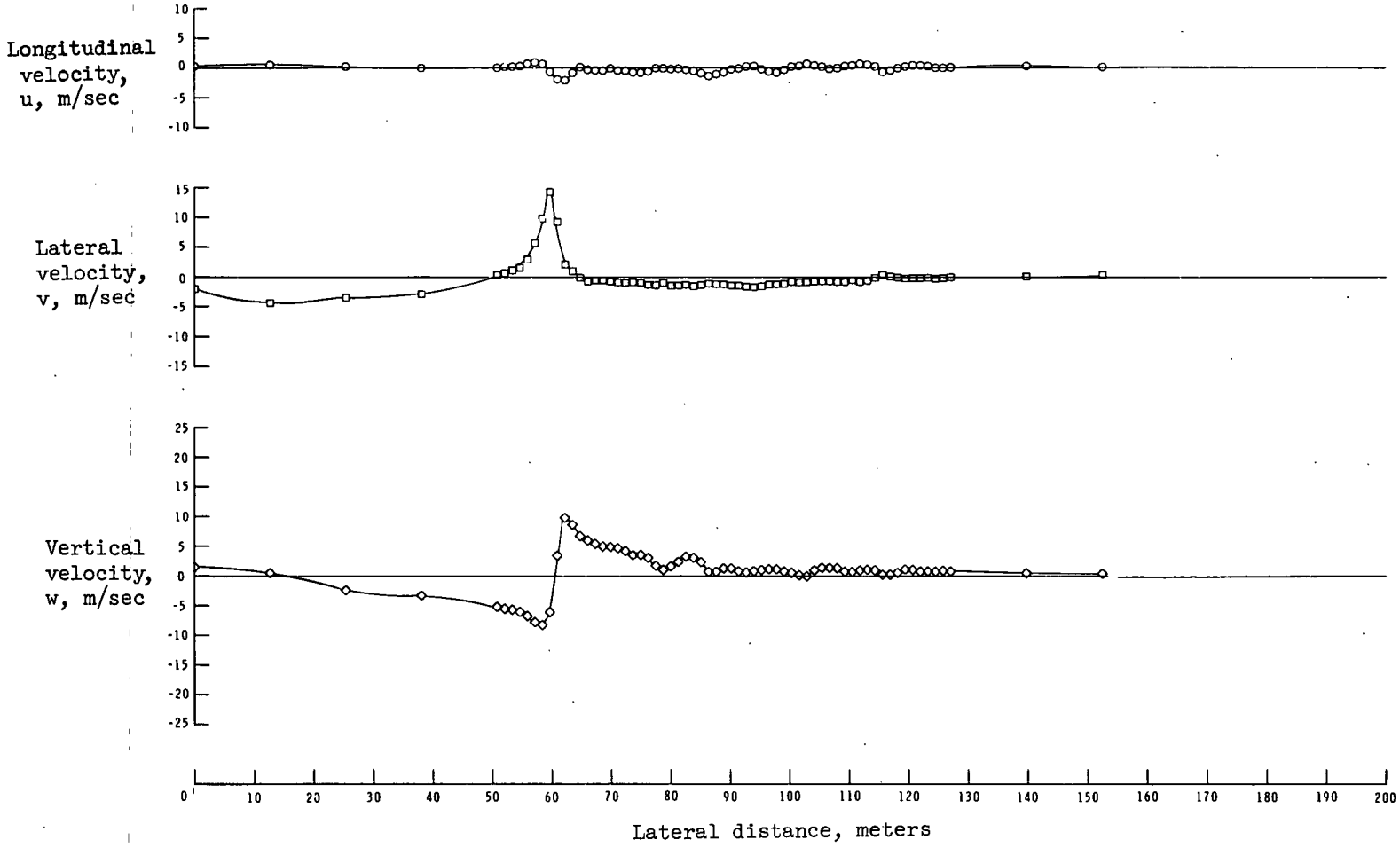

(b) t = 60 sec.

Figure 2.- Continued.

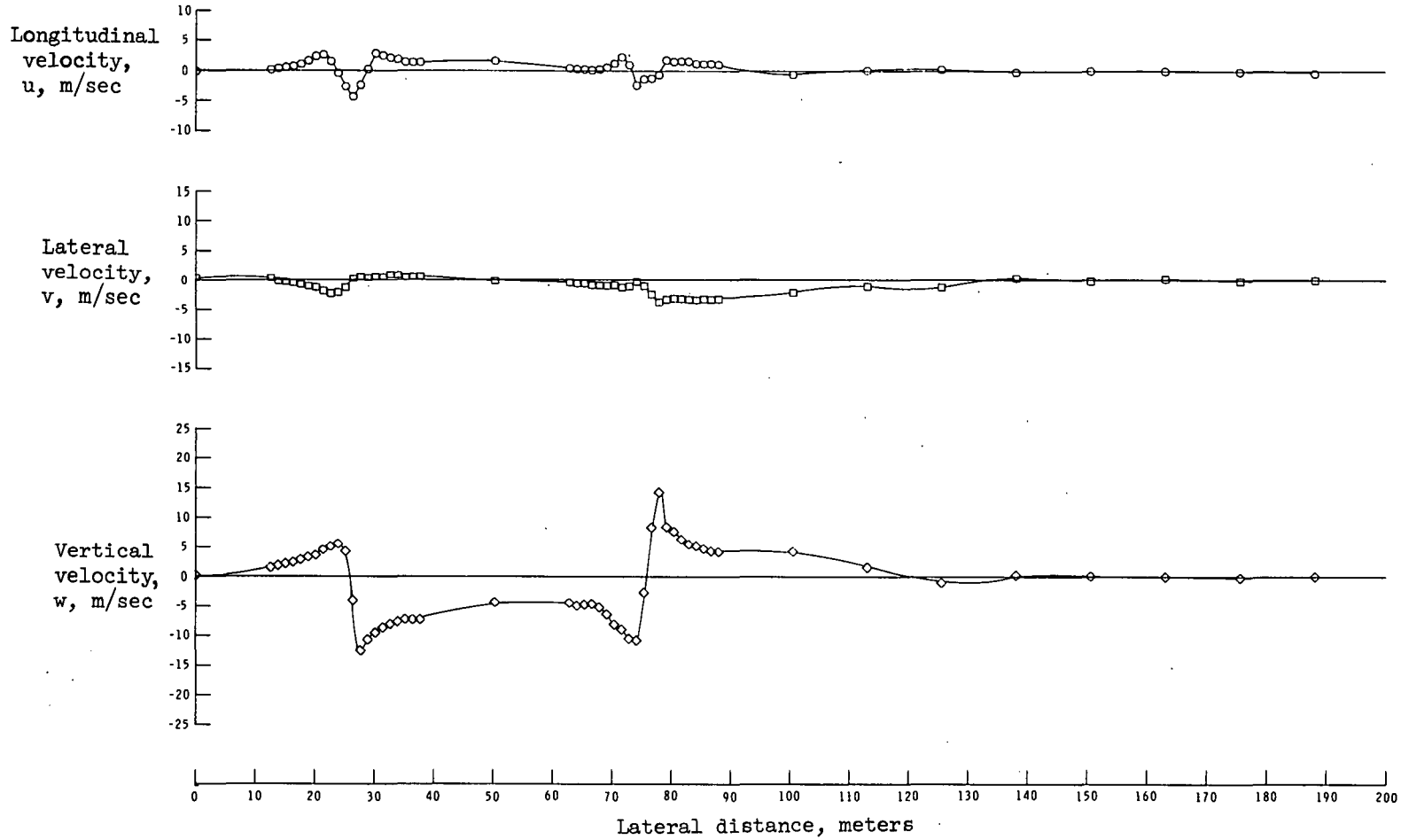

(c) t = 98 sec.

Figure 2.- Continued.

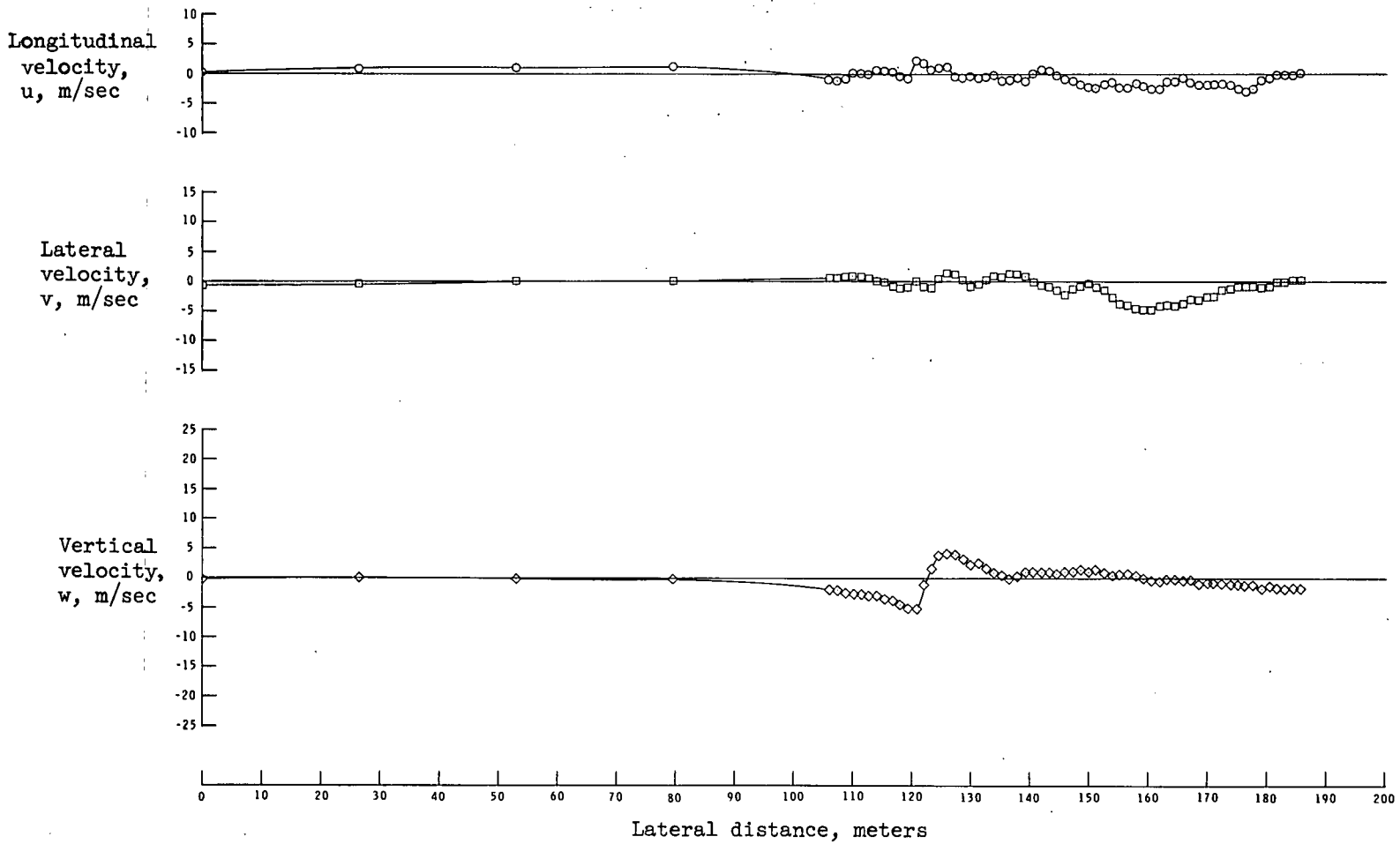

(d) t = 104 sec.

Figure 2.- Continued.

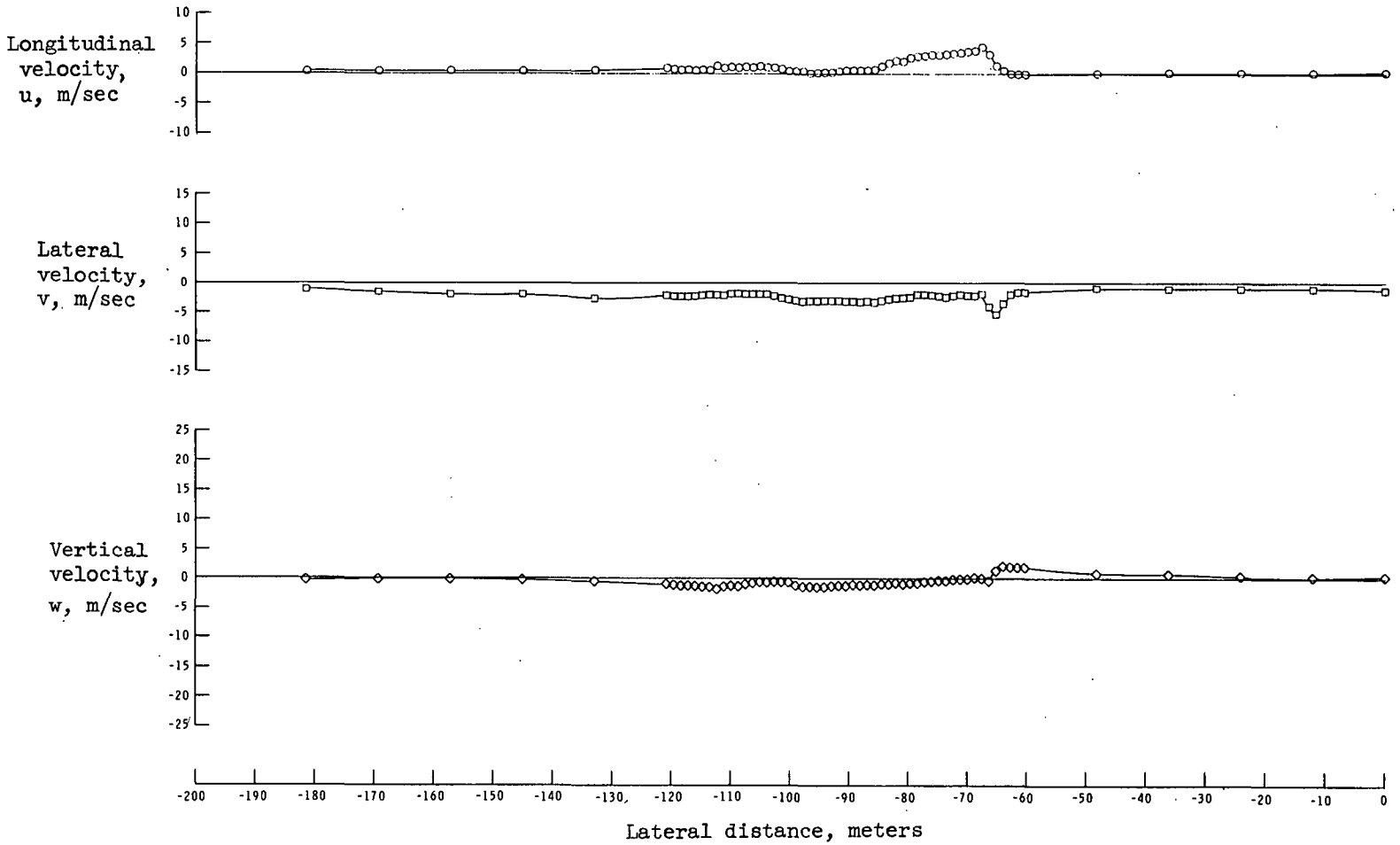

(e) t = 163 sec.

Figure 2.- Continued.

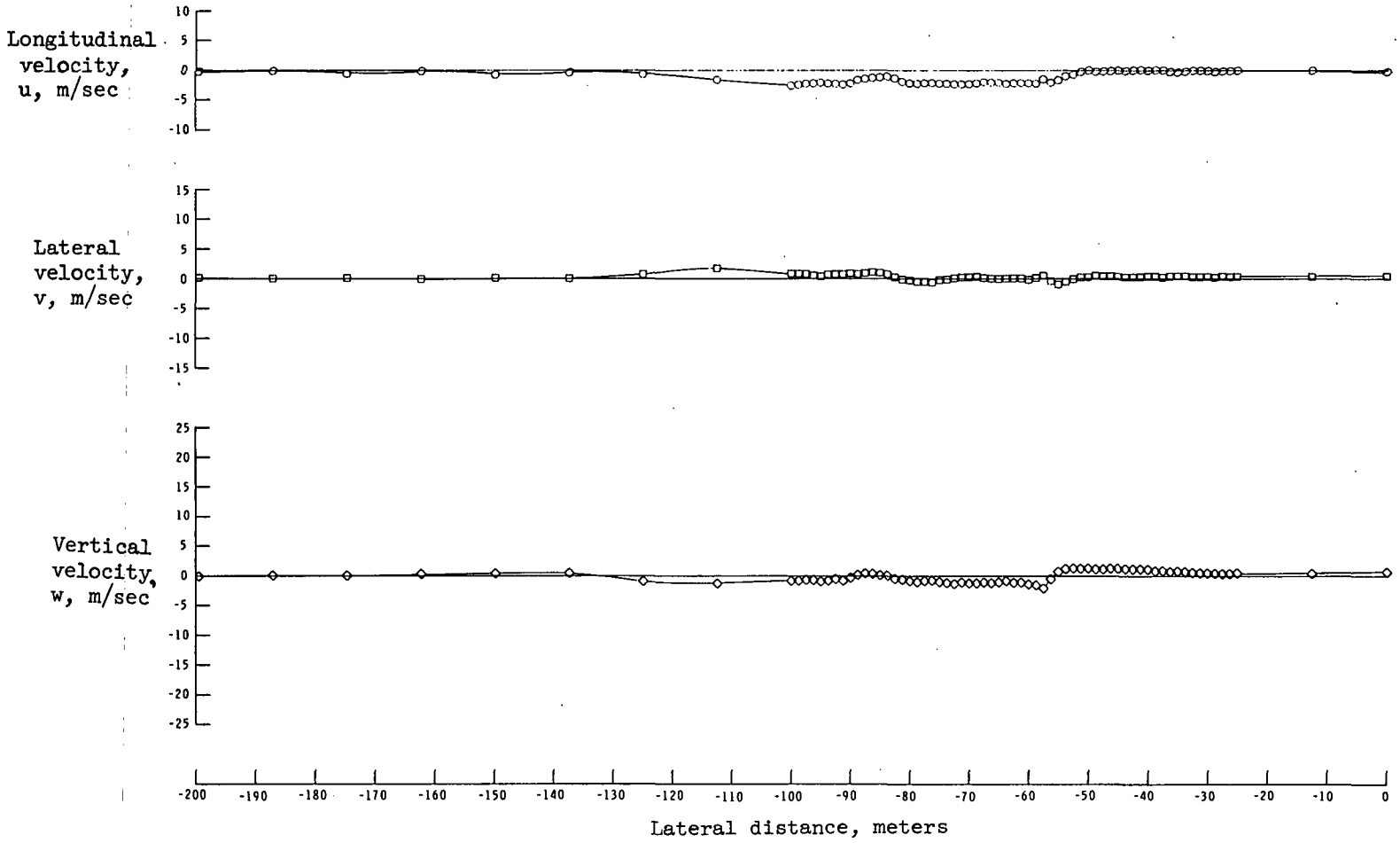

(f) t = 198 sec.

Figure 2.- Concluded.

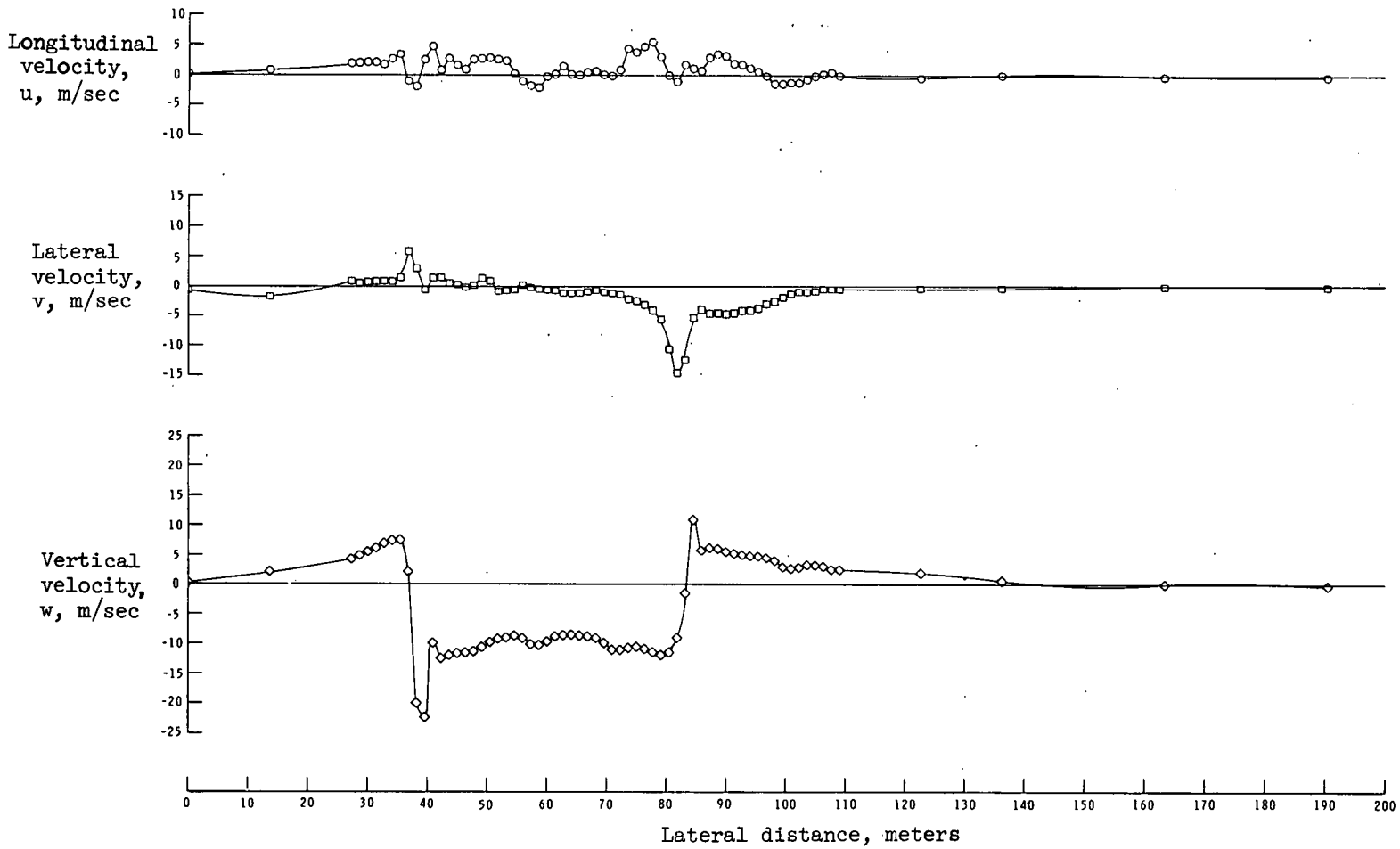

(a) t = 24 sec.

Figure 3.- Vortex velocity component variation with lateral distance. Flaps down.

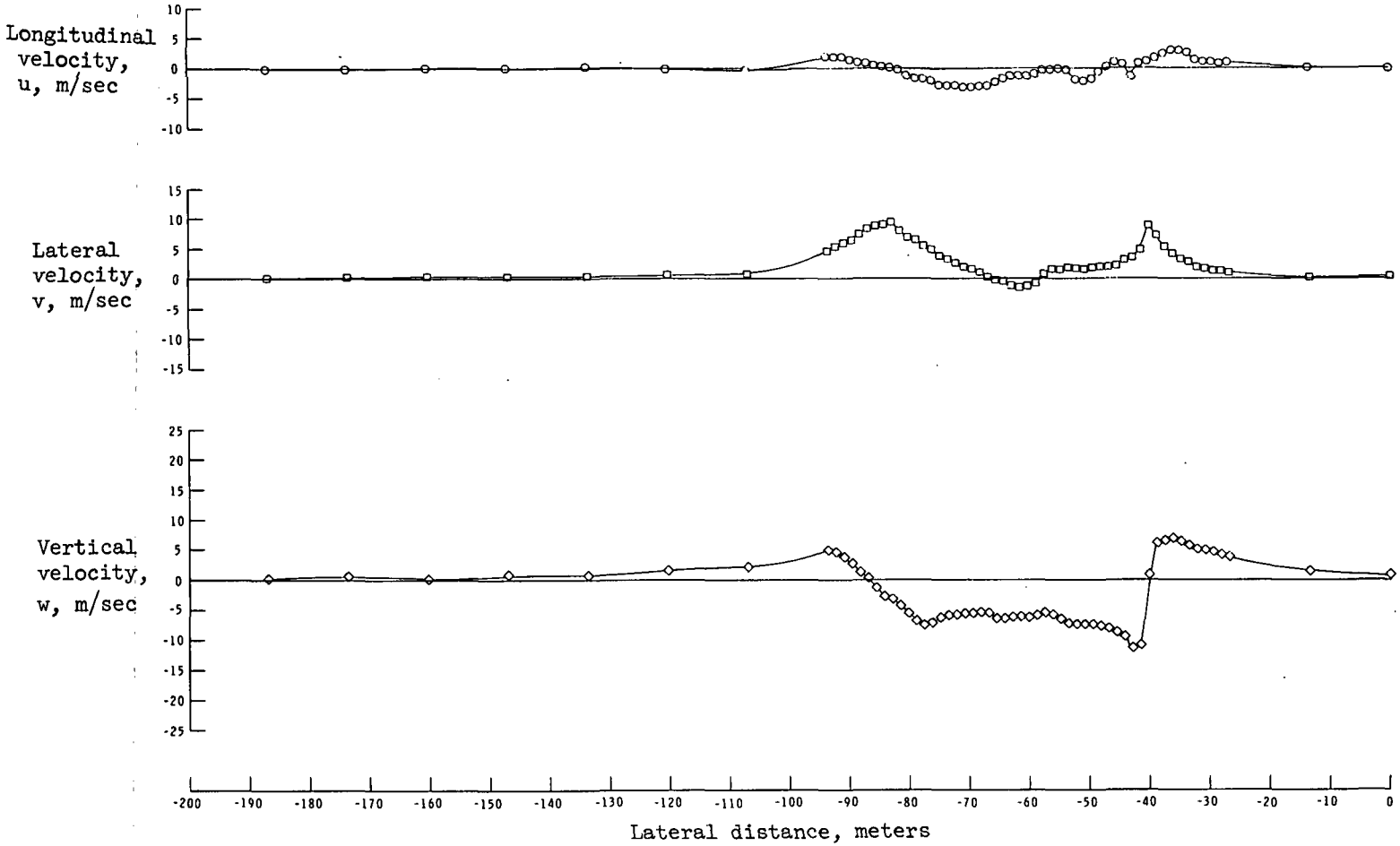

(b) t = 59 sec.

Figure 3.- Continued.

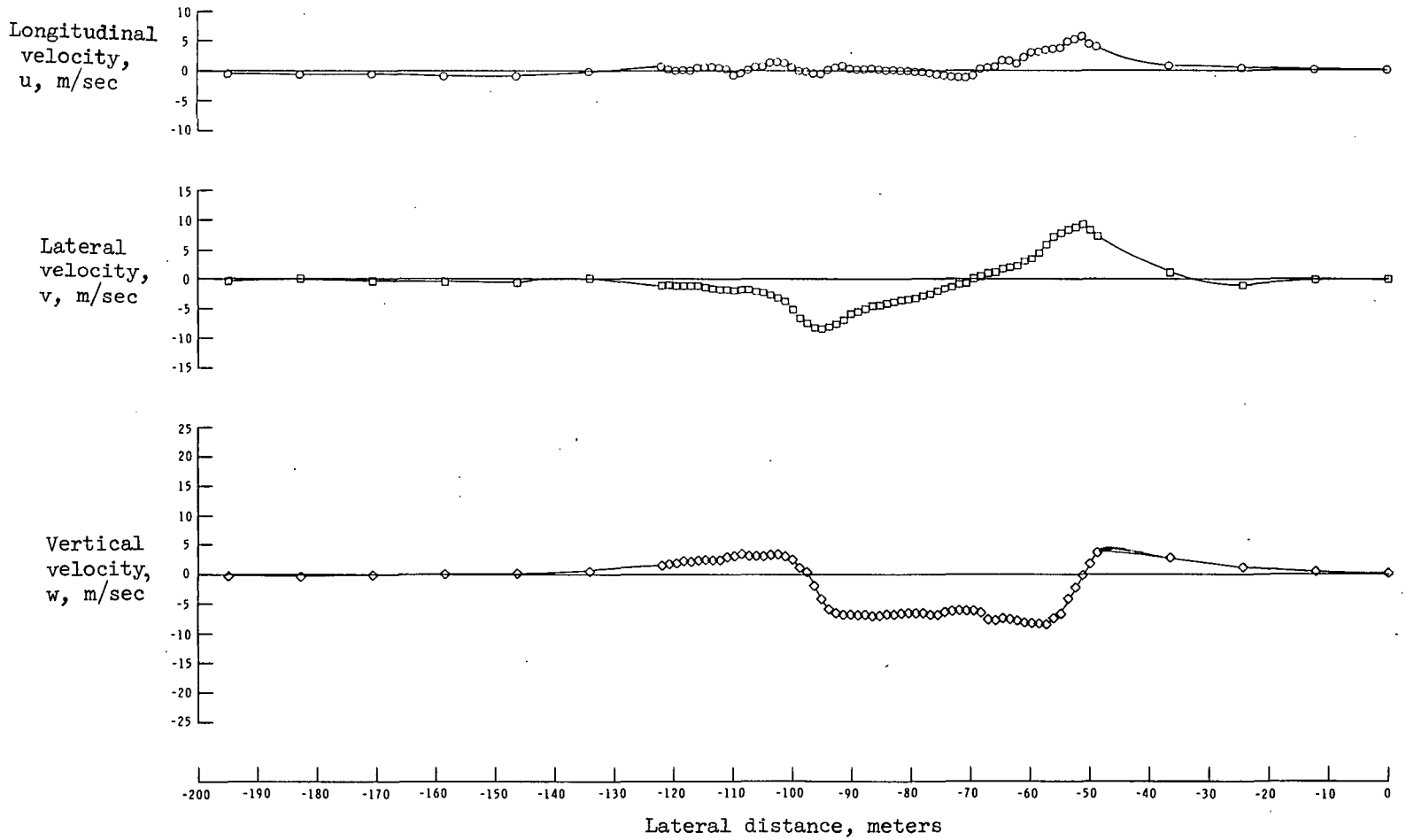

(c) t = 60 sec.

Figure 3.- Continued.

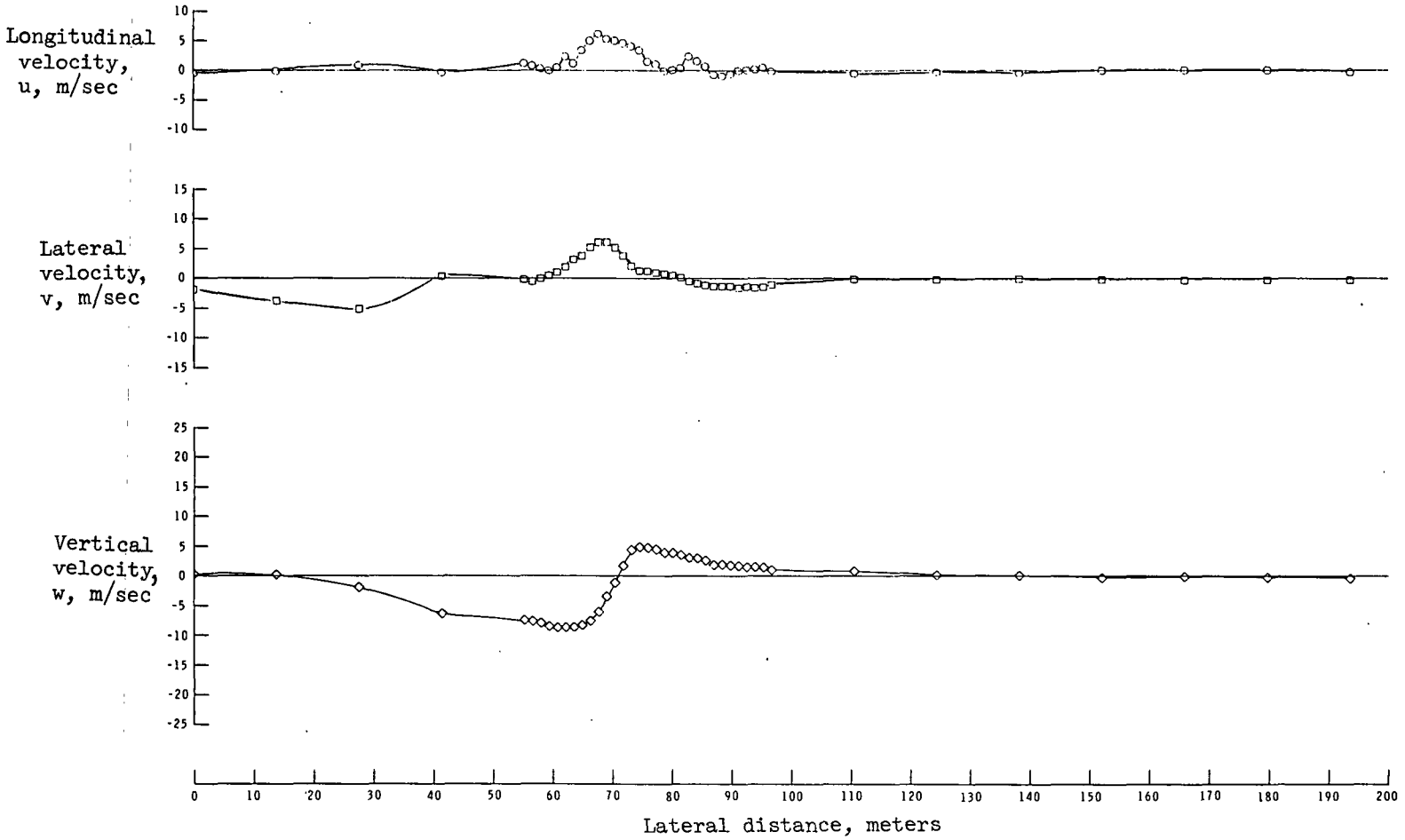

(d) t = 63 sec.

Figure 3.- Continued.

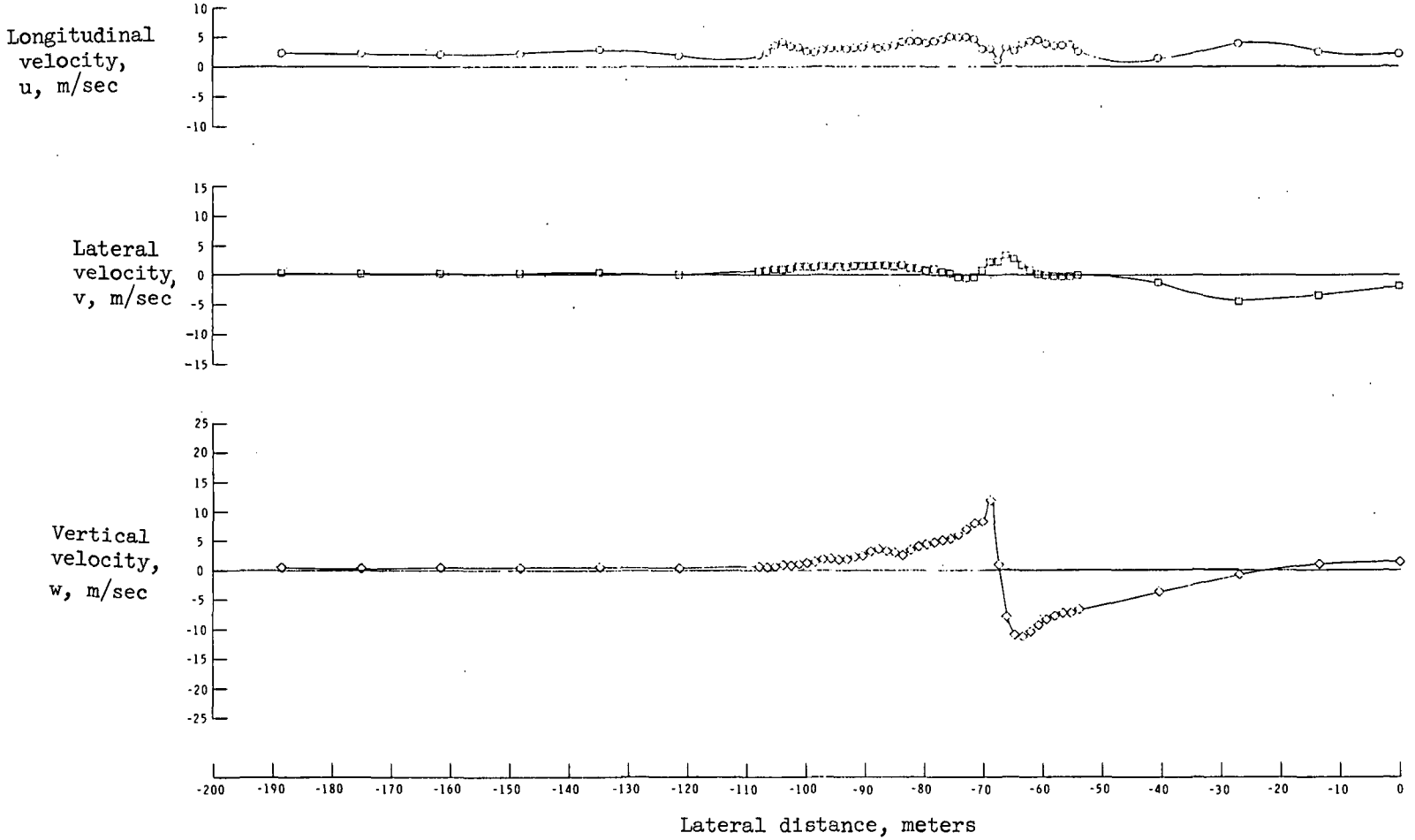

(e) t = 78 sec.

Figure 3.- Continued.

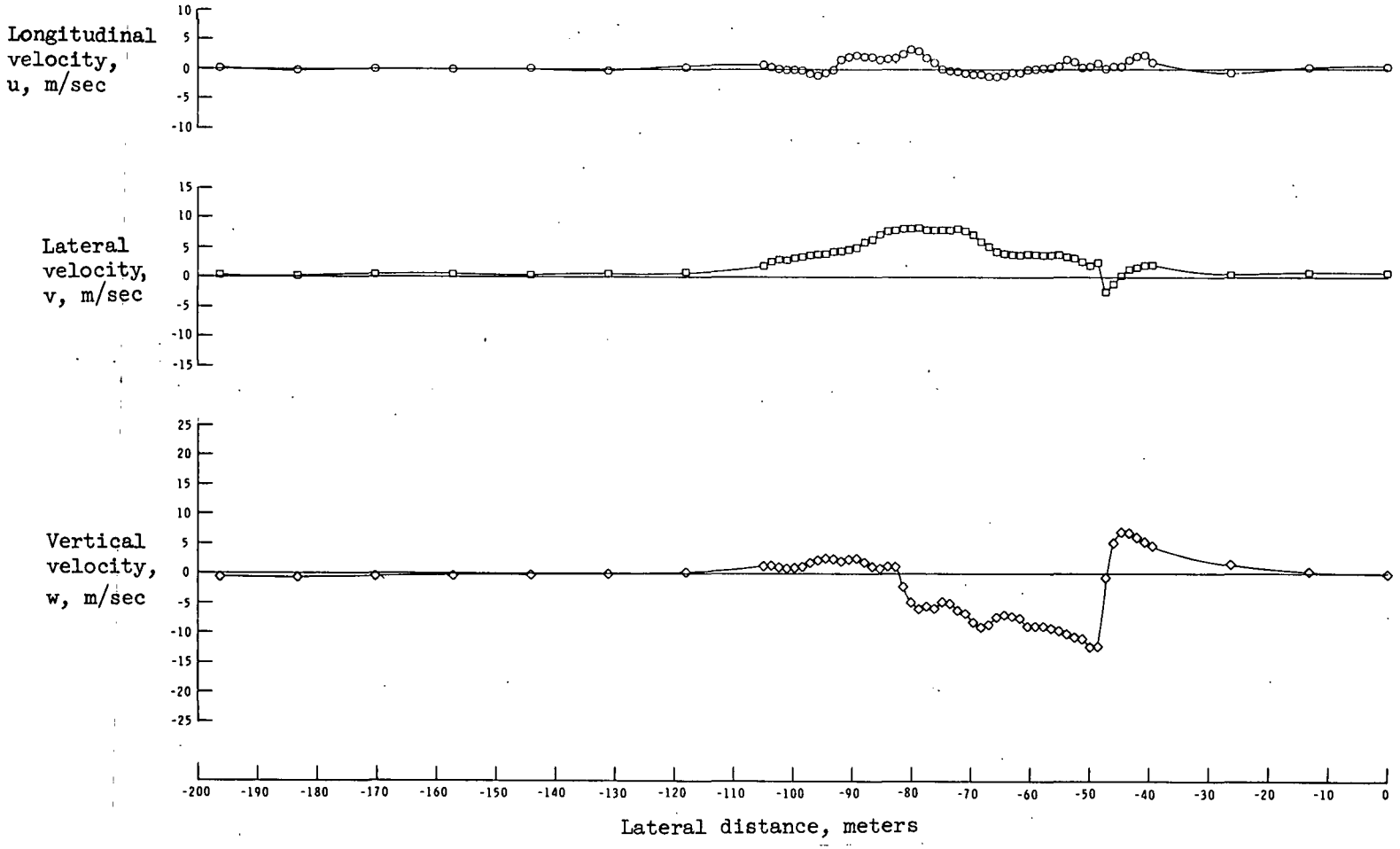

(f) t = 82 sec.

Figure 3.- Continued.

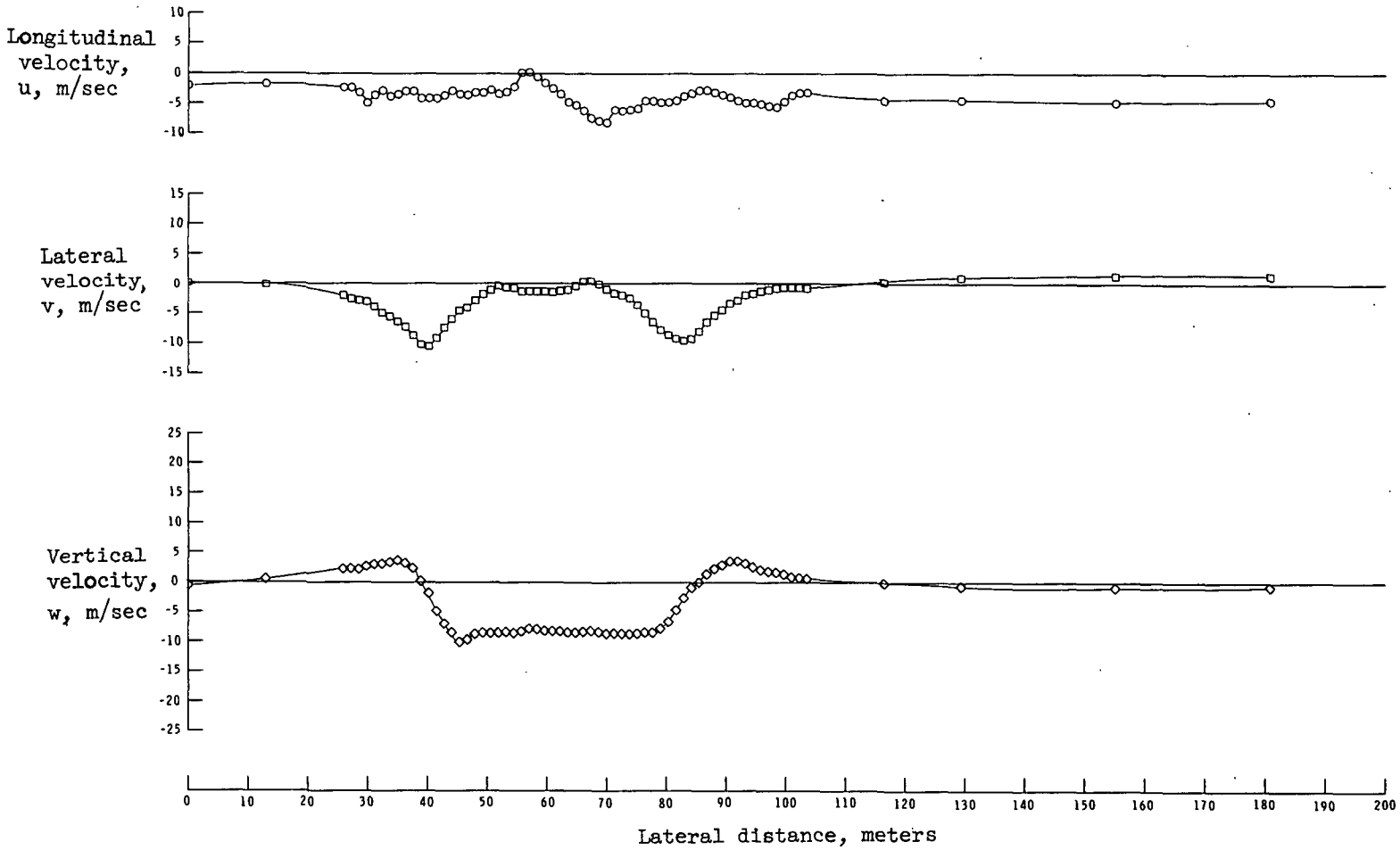

(g) t = 85 sec.

Figure 3.- Continued.

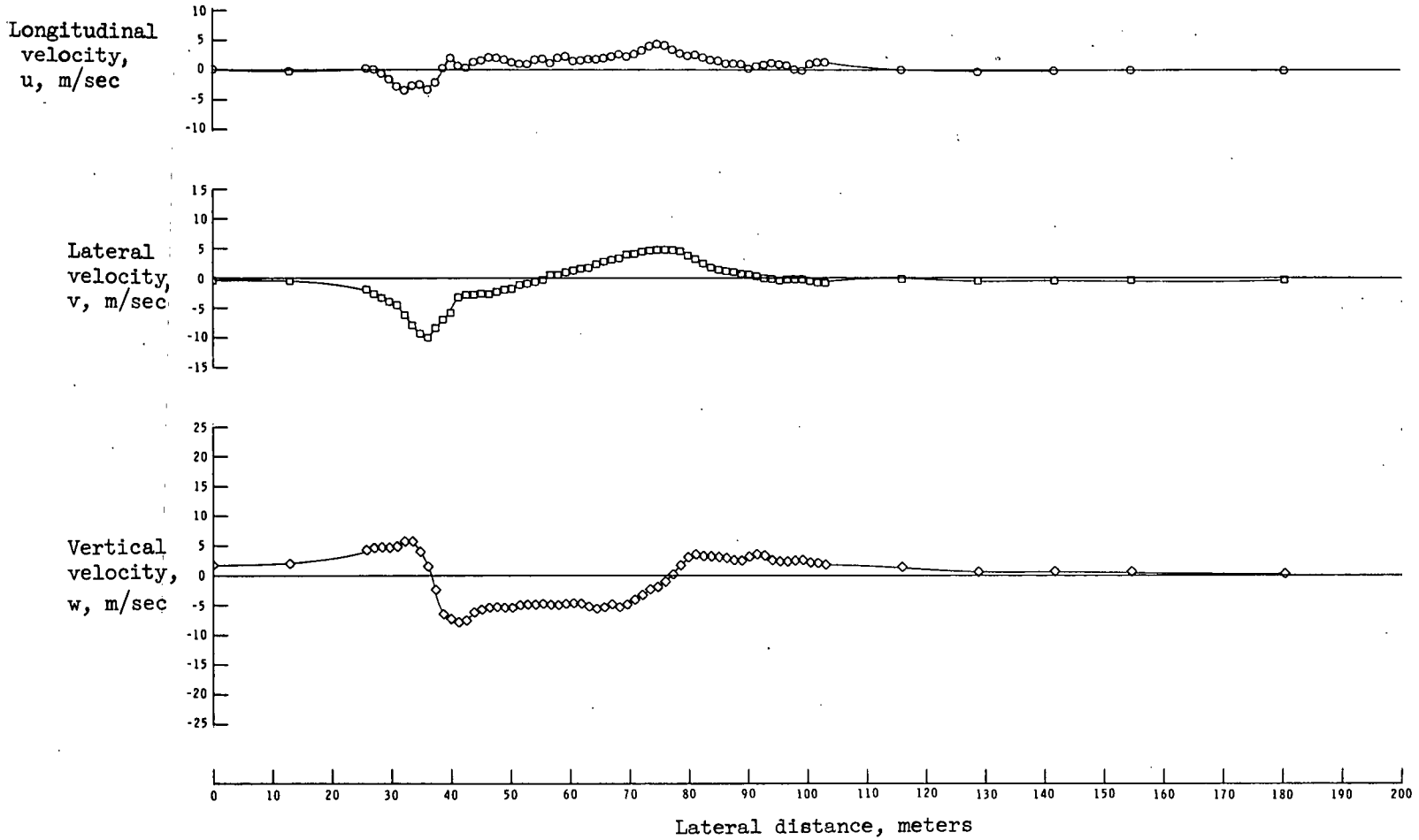

(h) t = 92 sec.

Figure 3.- Continued.

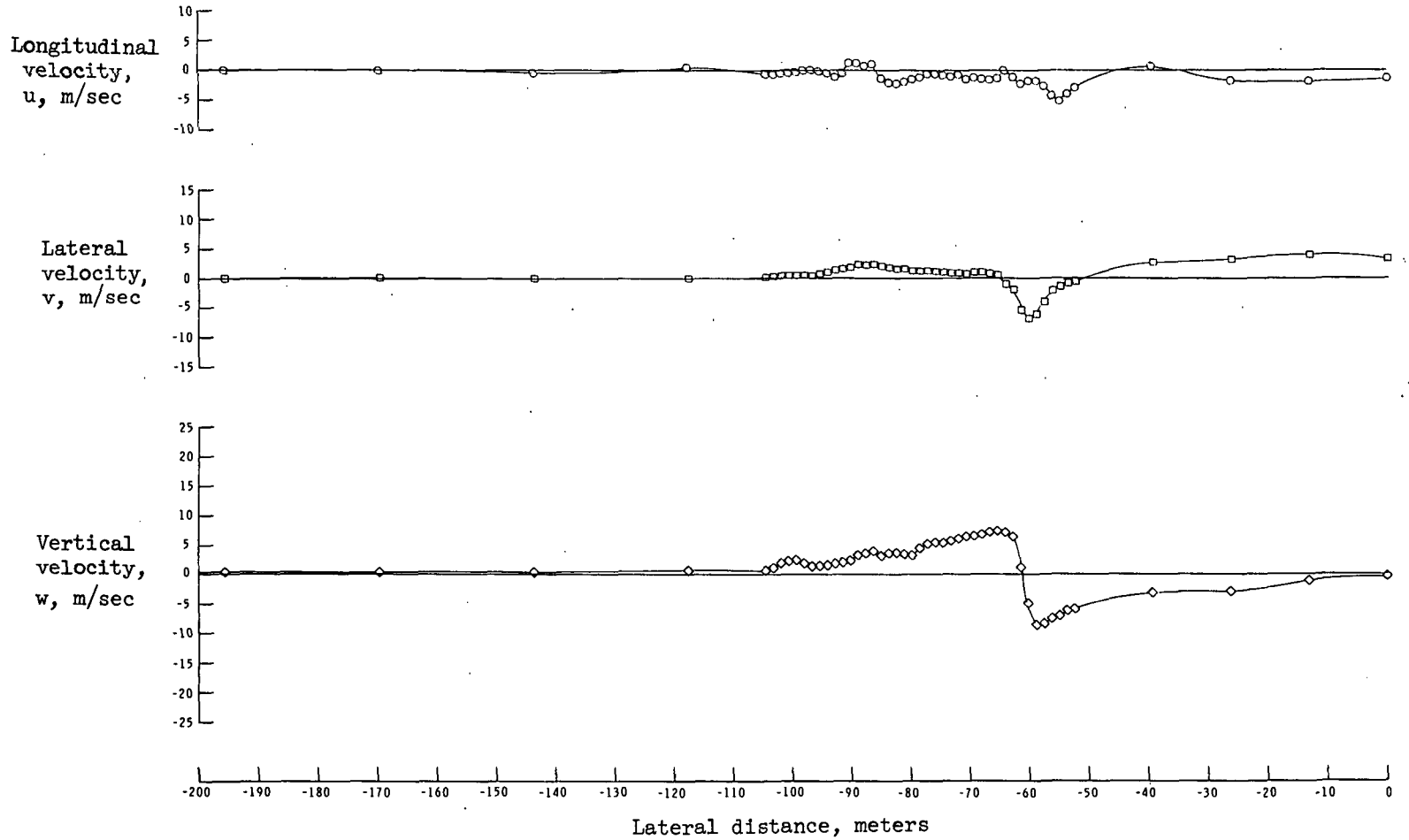

(i) t = 93 sec.

Figure 3.- Continued.

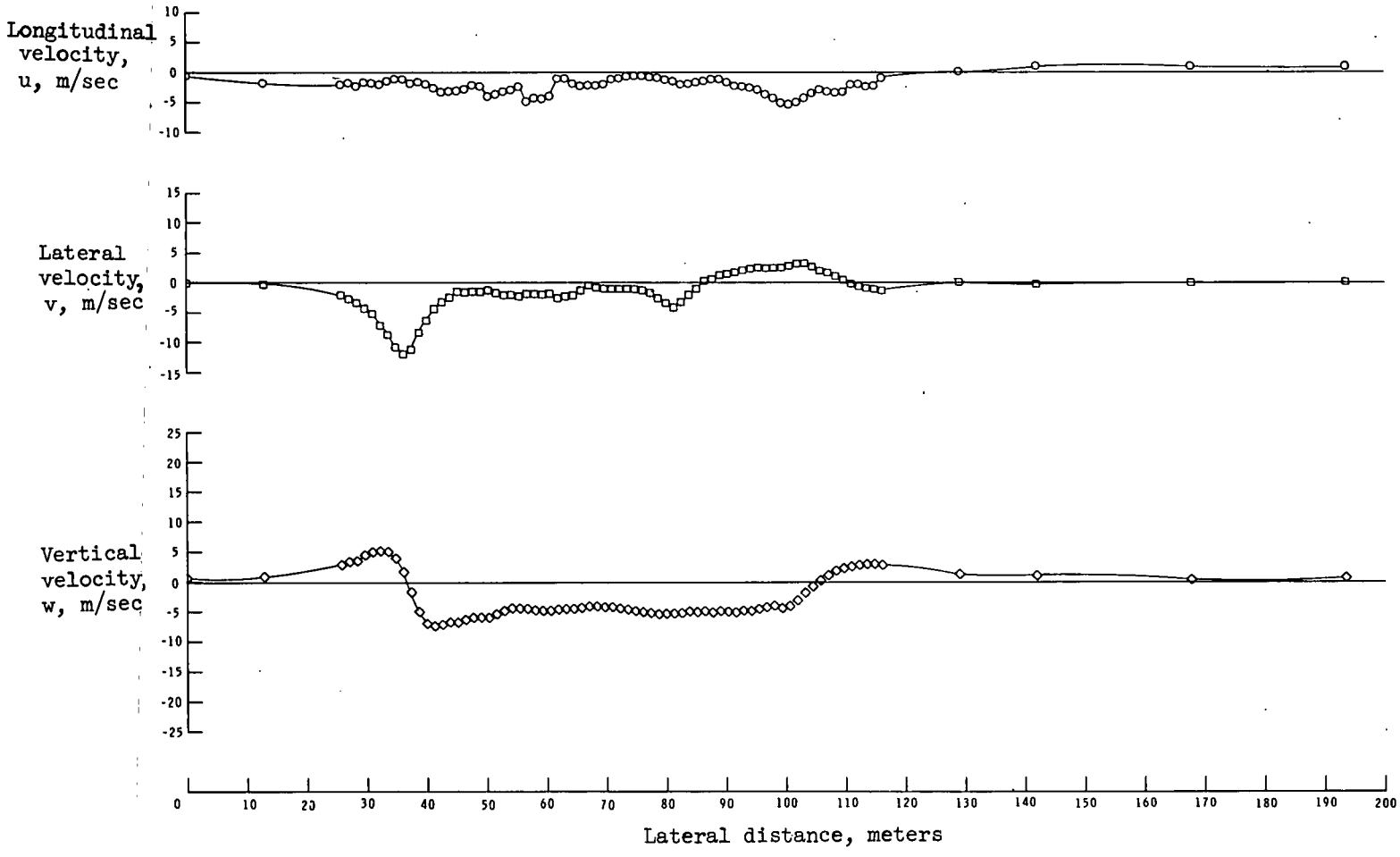

(j) t = 106 sec.

Figure 3.- Continued.

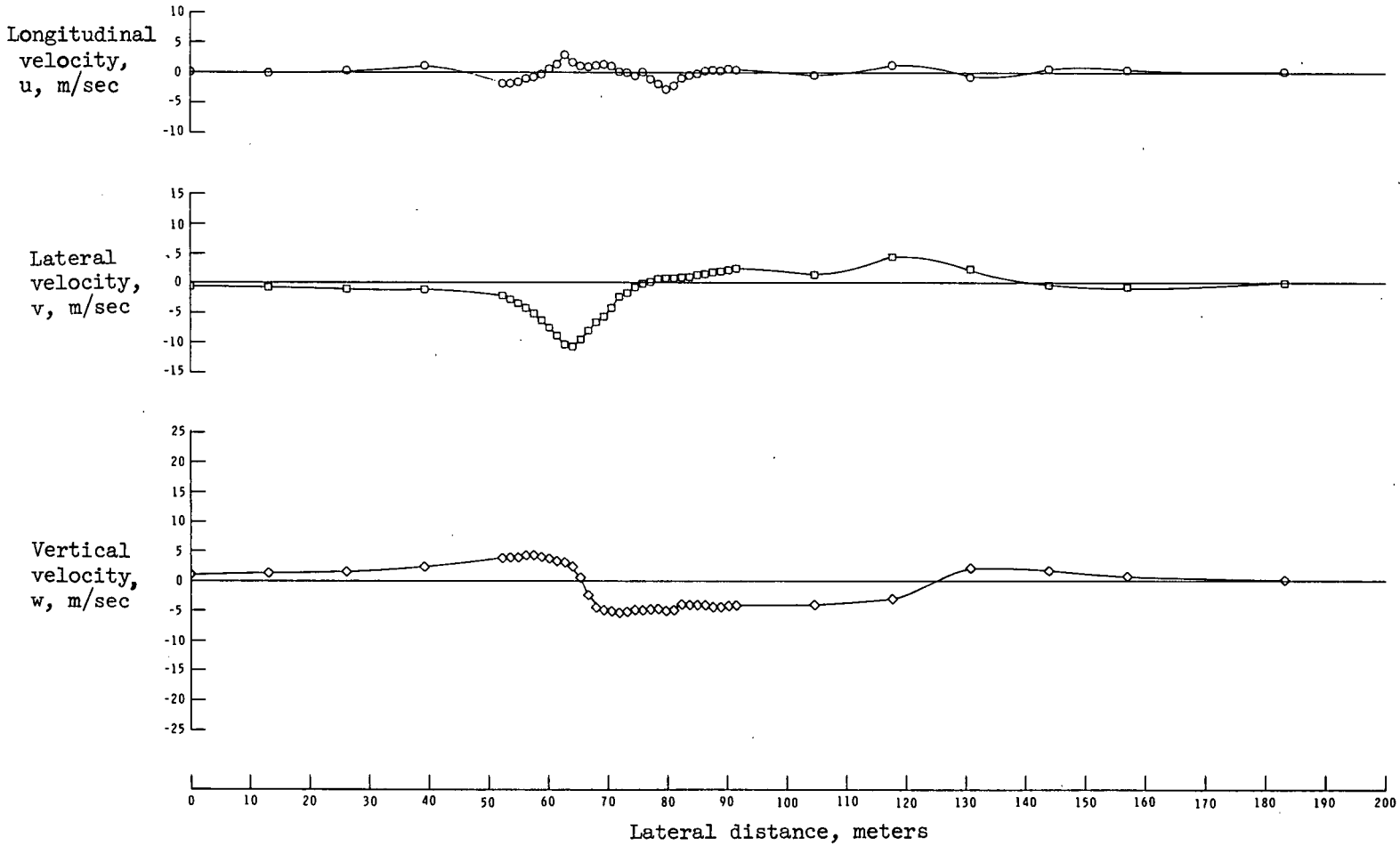

(k) t = 109 sec.

Figure 3.- Continued.

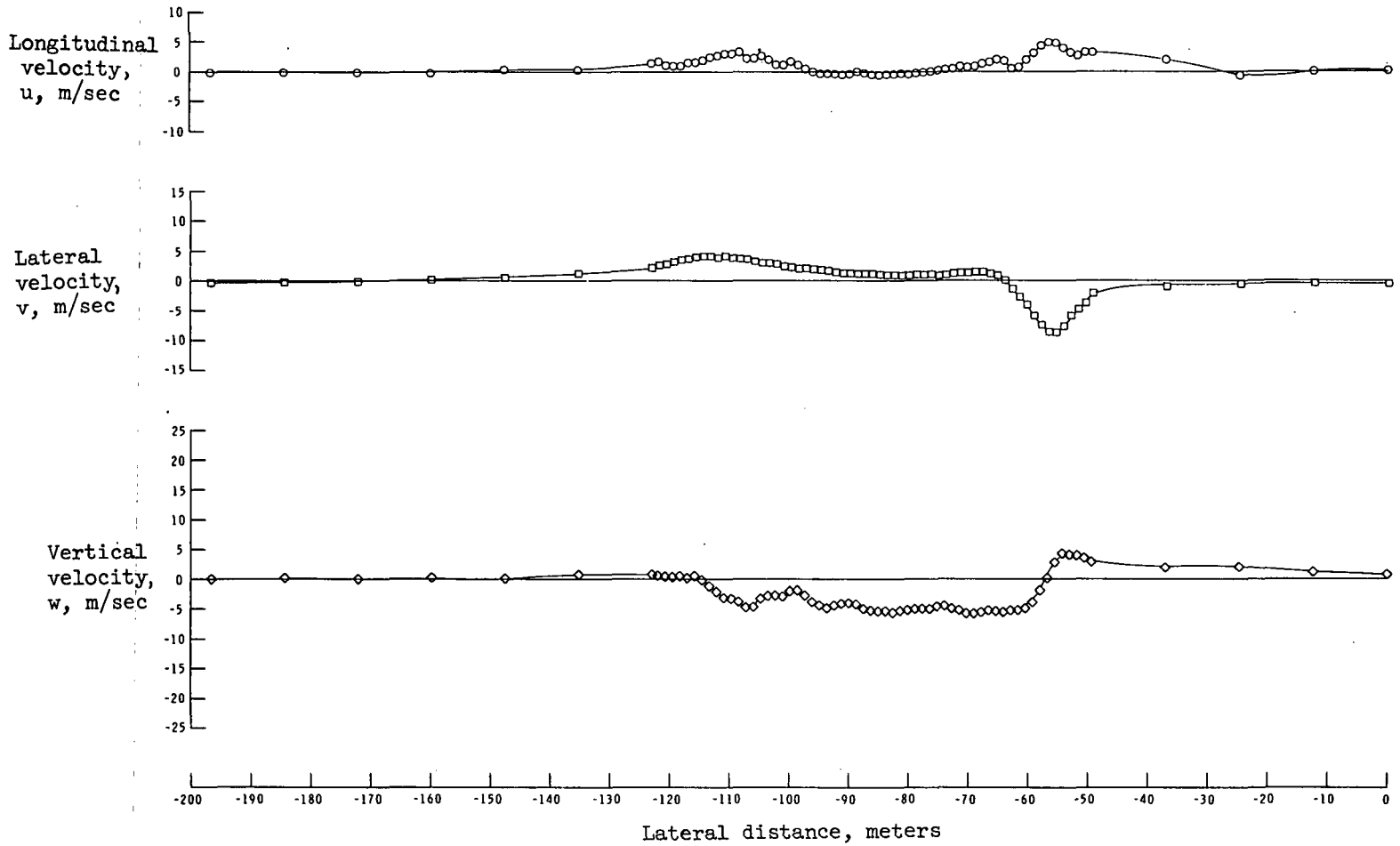

(l) t = 115 sec.

Figure 3.- Continued.

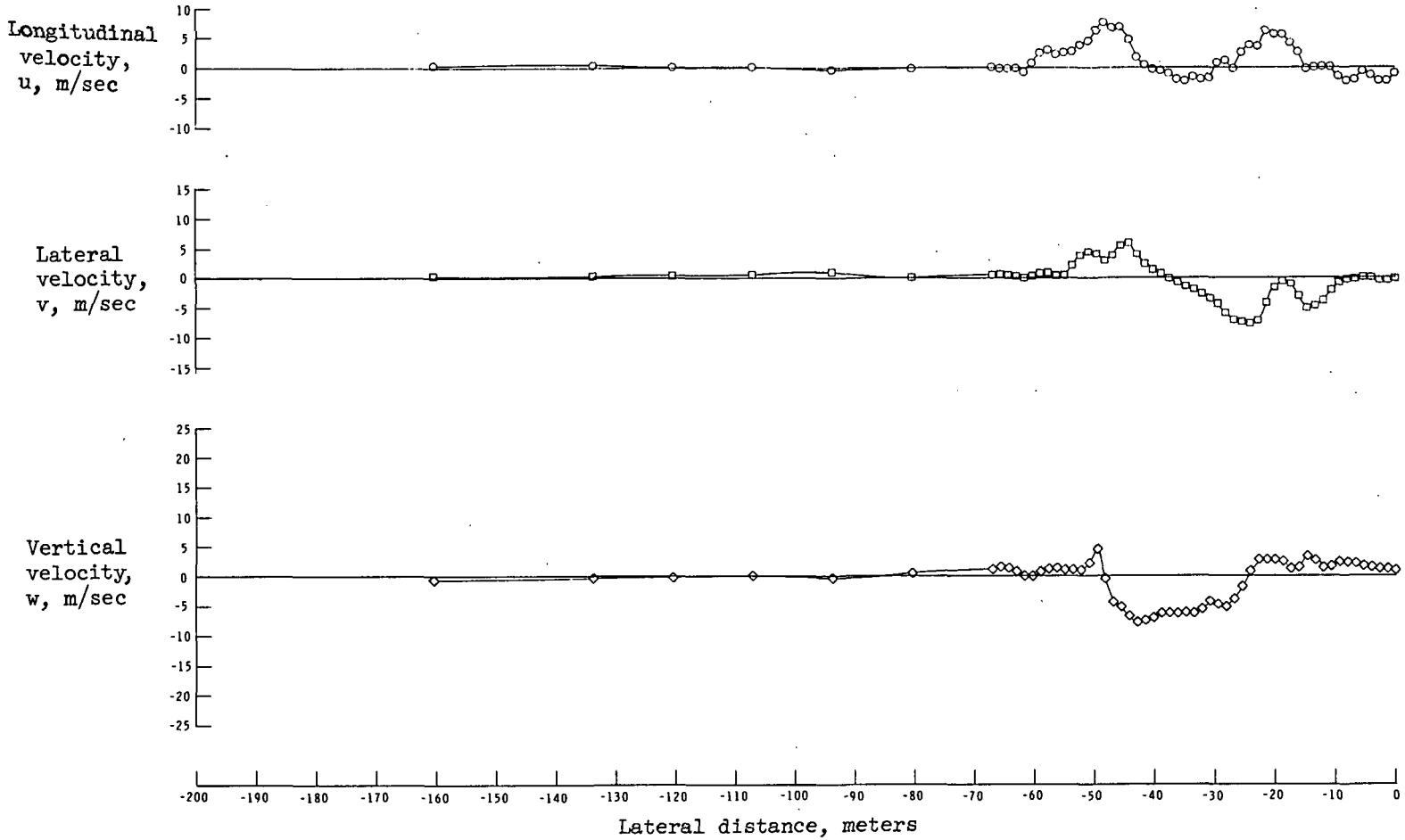

(m) t = 133 sec.

Figure 3.- Continued.

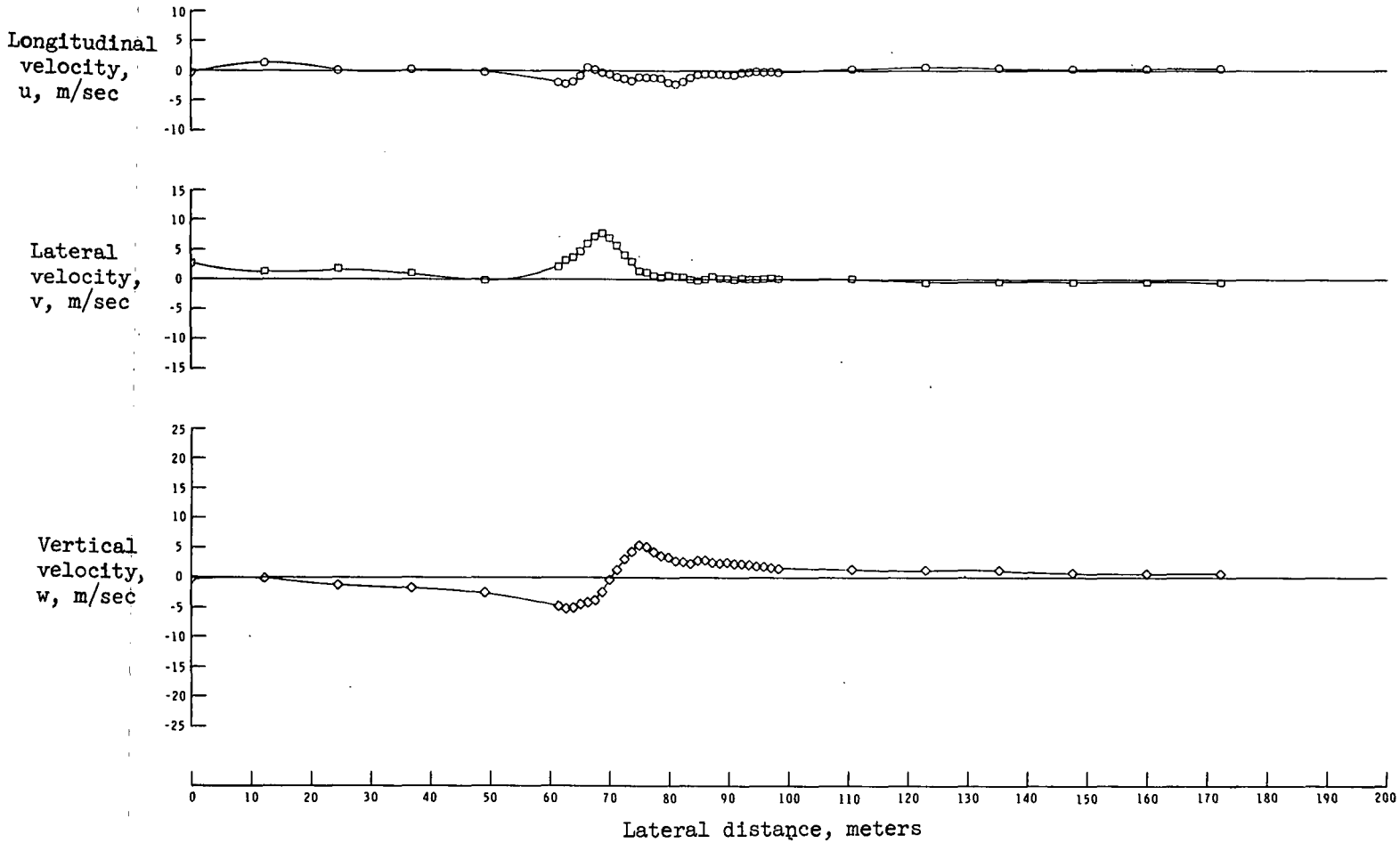

(n) t = 147 sec.

Figure 3.- Concluded.

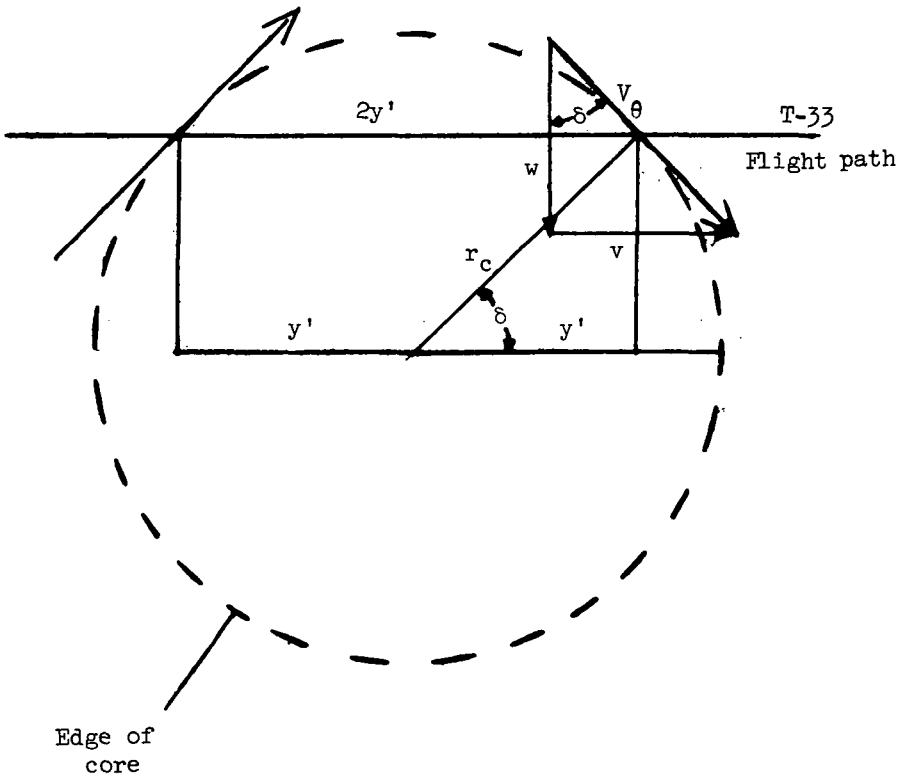

Figure 4.- Experimental determination of core radius. $r_c = y' \frac{V_\theta}{w}$.

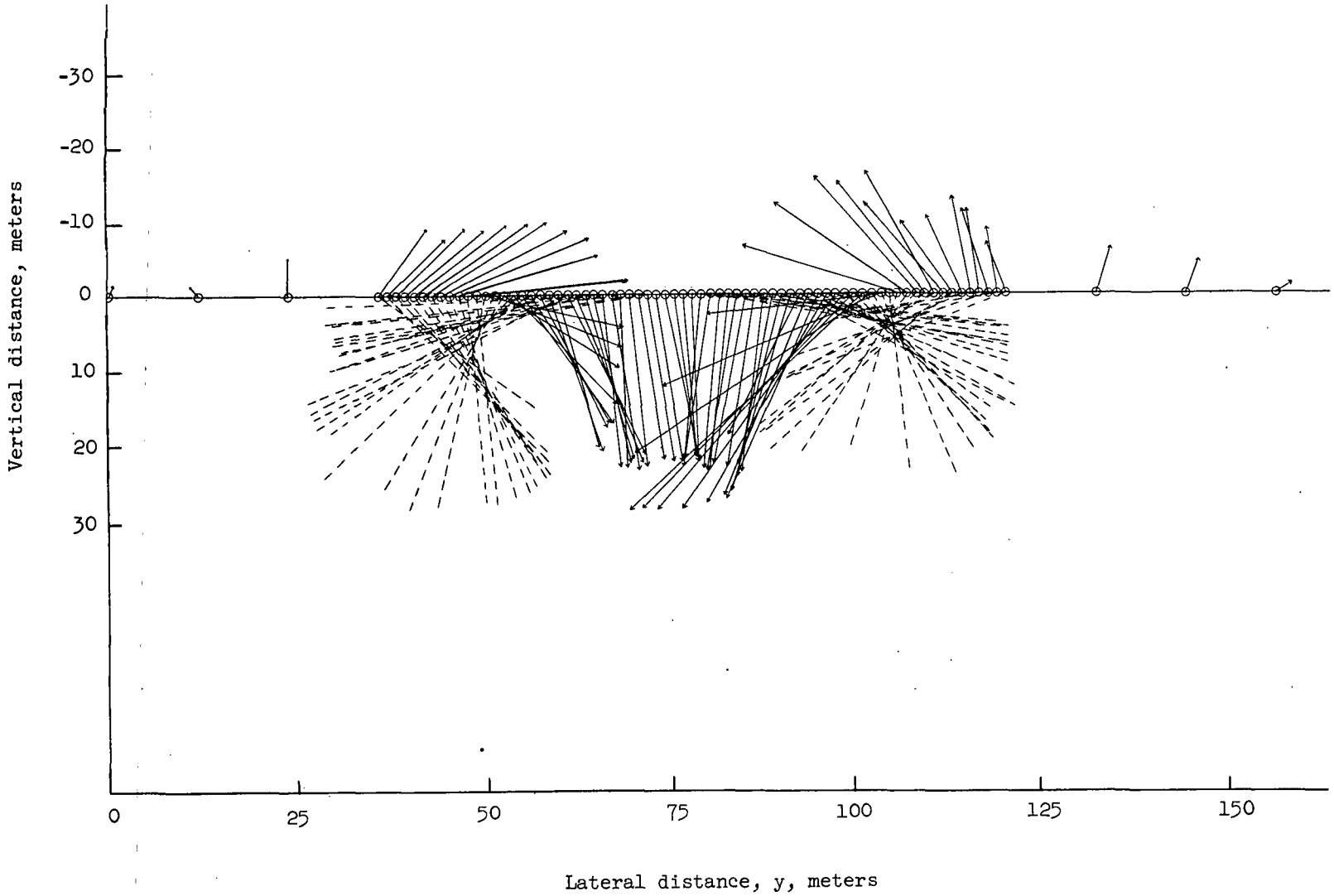

Figure 5.- Experimental determination of core locations.

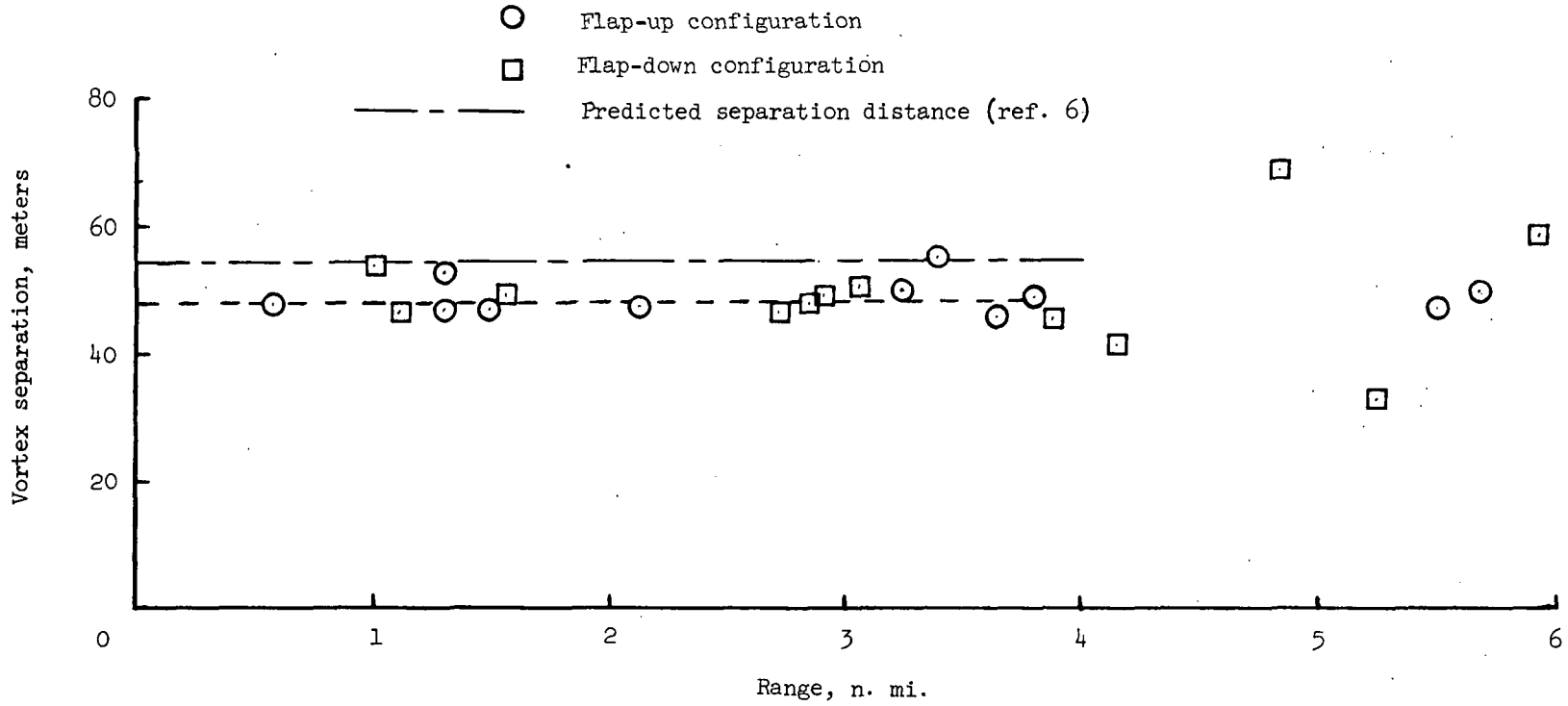

Figure 6.- Lateral vortex spacing.

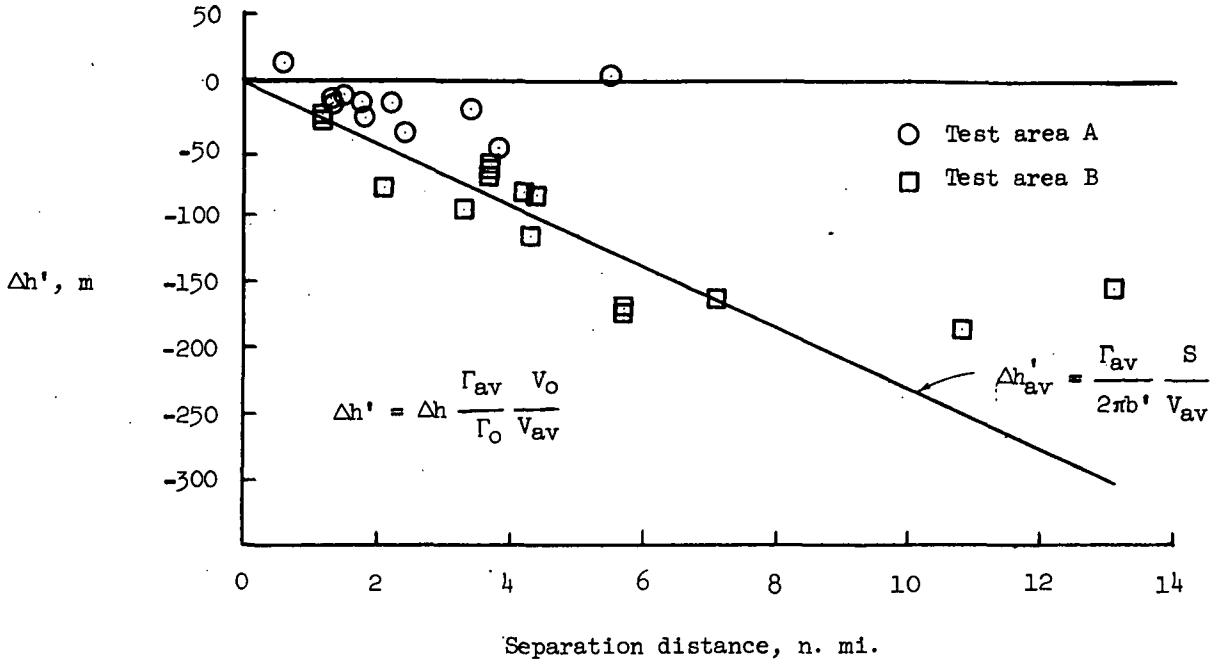

(a) Flaps up; Γ_{av} = 462.6 m^2/sec; V_{av} = 110.58 m^2/sec.

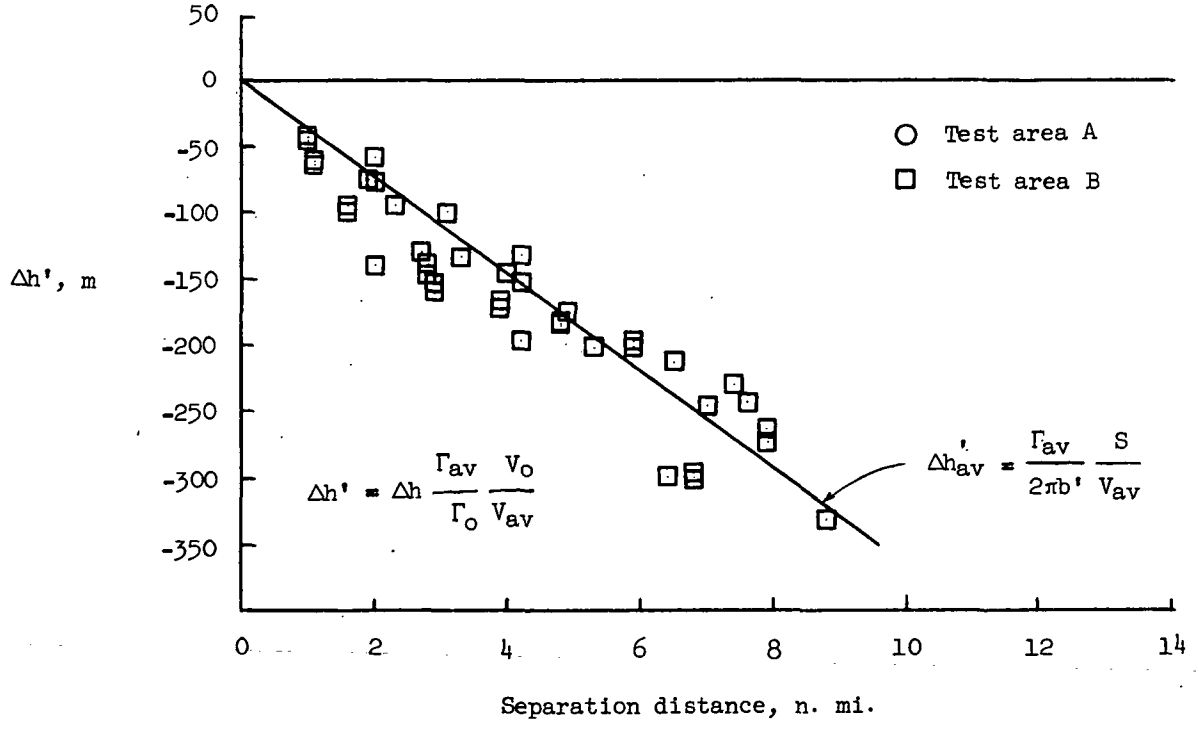

(b) Flaps down; Γ_{av} = 591.8 m^2/sec; V_{av} = 89.37 m^2/sec.

Figure 7.- Vortex vertical positions.

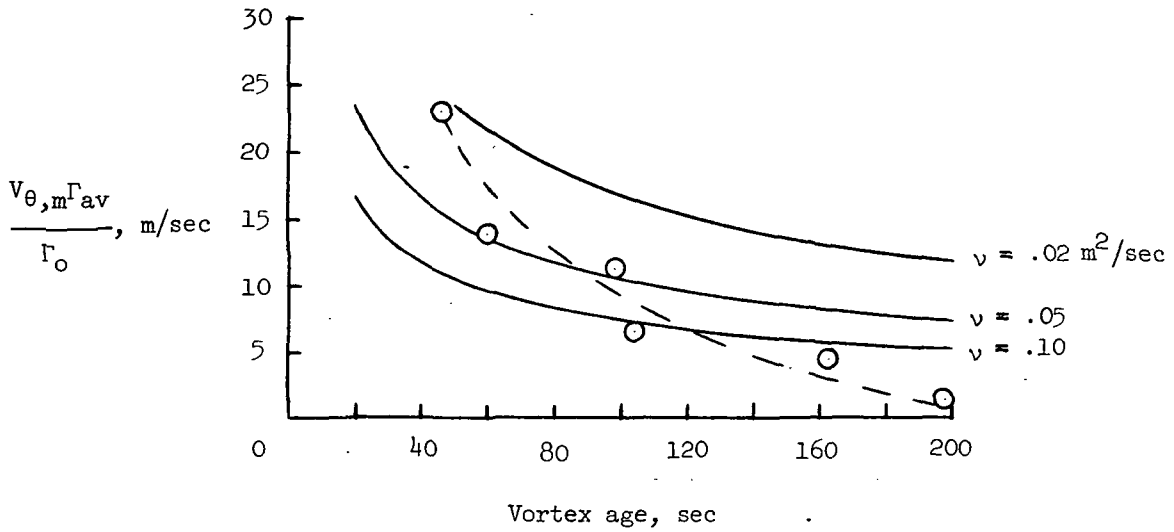

(a) Flap-up configuration; Γ_{av} = 462.6 m^2/sec.

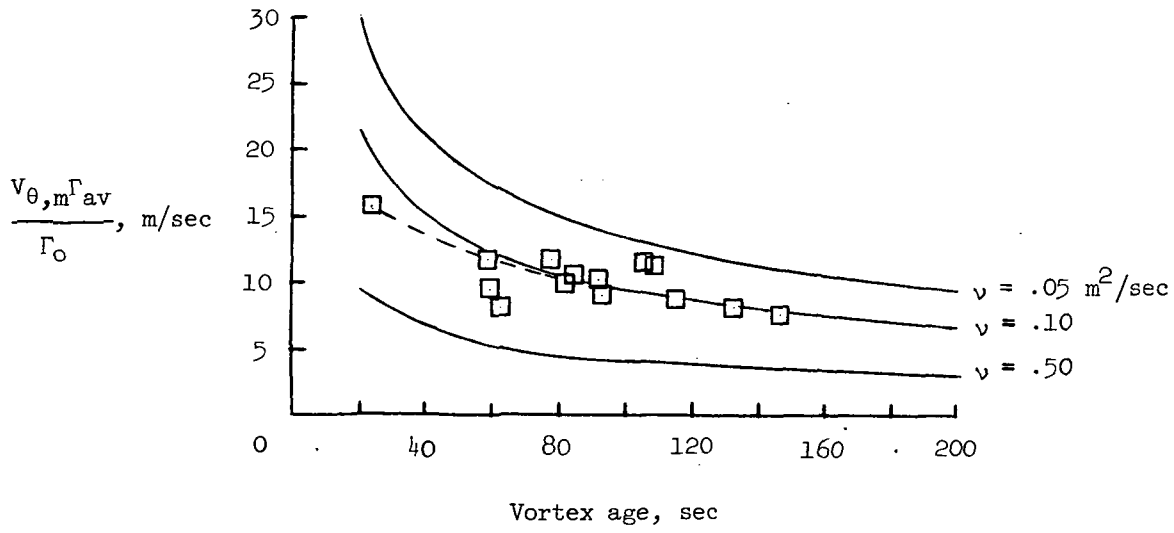

(b) Flap-down configuration; Γ_{av} = 591.8 m^2/sec.

Figure 8.- Variation of maximum longitudinal velocity with vortex age.

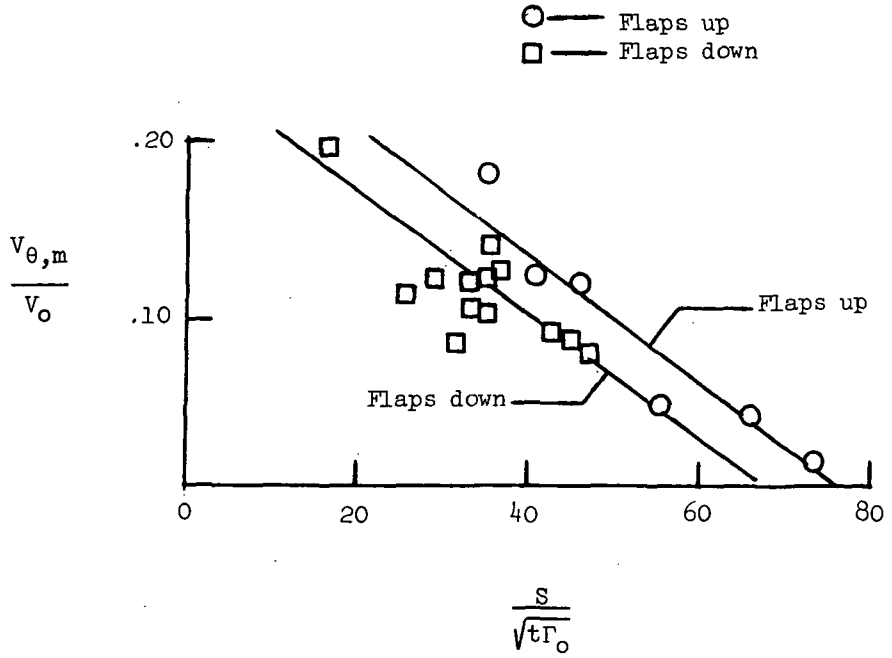

Figure 9.- Nondimensional variation of vortex velocity with separation distance.

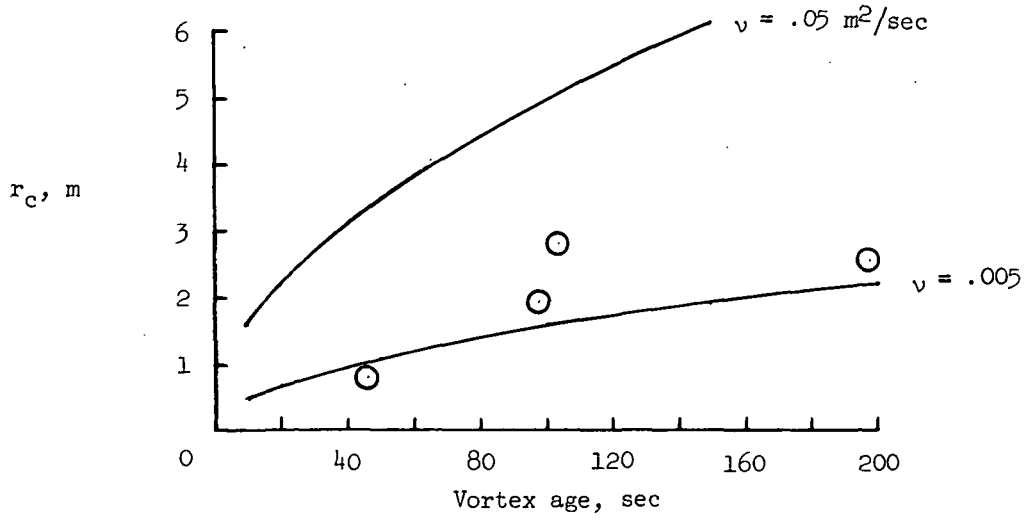

(a) Flap-up configuration.

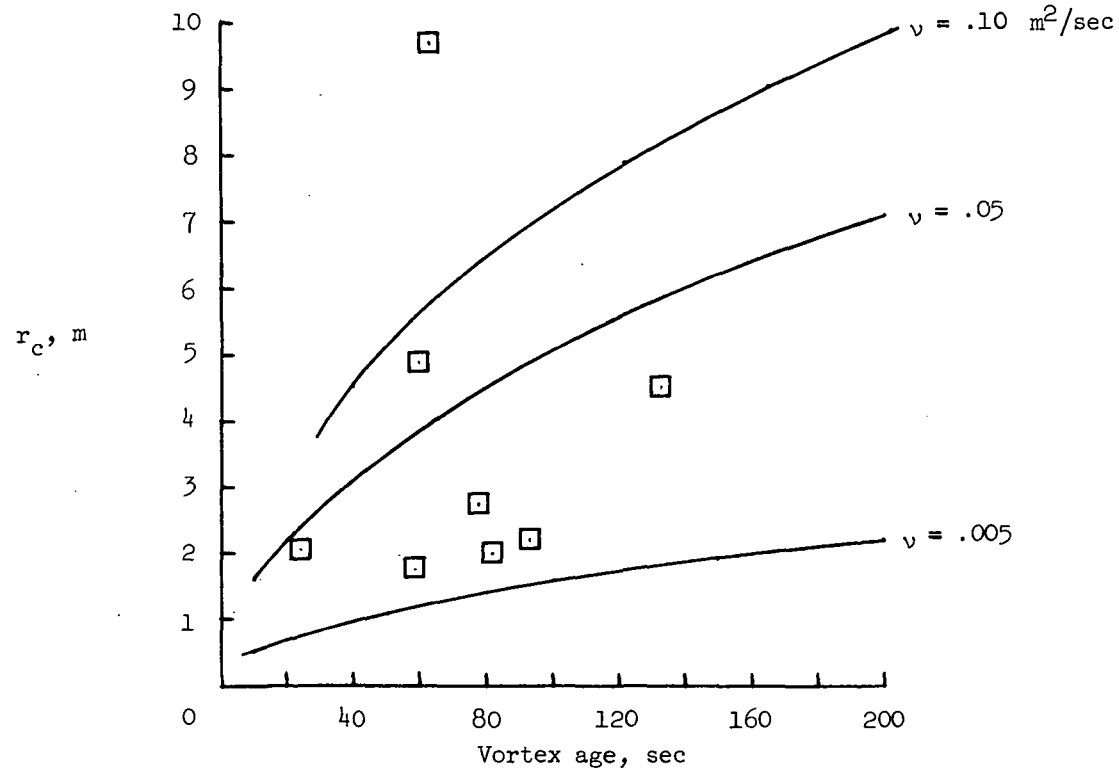

(b) Flap-down configuration.

Figure 10.- Variation of core radius with vortex age.

NASA-Langley, 1973 — 2 L-8706

NATIONAL AERONAUTICS AND SPACE ADMINISTRATION
WASHINGTON, D.C. 20546

OFFICIAL BUSINESS
PENALTY FOR PRIVATE USE $300

SPECIAL FOURTH-CLASS RATE
BOOK

POSTAGE AND FEES PAID
NATIONAL AERONAUTICS AND
SPACE ADMINISTRATION
451

U.S.MAIL

POSTMASTER: If Undeliverable (Section 158 Postal Manual) Do Not Return

"The aeronautical and space activities of the United States shall be conducted so as to contribute . . . to the expansion of human knowledge of phenomena in the atmosphere and space. The Administration shall provide for the widest practicable and appropriate dissemination of information concerning its activities and the results thereof."

—NATIONAL AERONAUTICS AND SPACE ACT OF 1958

NASA SCIENTIFIC AND TECHNICAL PUBLICATIONS

TECHNICAL REPORTS: Scientific and technical information considered important, complete, and a lasting contribution to existing knowledge.

TECHNICAL NOTES: Information less broad in scope but nevertheless of importance as a contribution to existing knowledge.

TECHNICAL MEMORANDUMS: Information receiving limited distribution because of preliminary data, security classification, or other reasons. Also includes conference proceedings with either limited or unlimited distribution.

CONTRACTOR REPORTS: Scientific and technical information generated under a NASA contract or grant and considered an important contribution to existing knowledge.

TECHNICAL TRANSLATIONS: Information published in a foreign language considered to merit NASA distribution in English.

SPECIAL PUBLICATIONS: Information derived from or of value to NASA activities. Publications include final reports of major projects, monographs, data compilations, handbooks, sourcebooks, and special bibliographies.

TECHNOLOGY UTILIZATION PUBLICATIONS: Information on technology used by NASA that may be of particular interest in commercial and other non-aerospace applications. Publications include Tech Briefs, Technology Utilization Reports and Technology Surveys.

Details on the availability of these publications may be obtained from:

SCIENTIFIC AND TECHNICAL INFORMATION OFFICE

NATIONAL AERONAUTICS AND SPACE ADMINISTRATION

Washington, D.C. 20546